Cellular Oncology (2025) 48:743–760
https://doi.org/10.1007/s13402-025-01044-x

RESEARCH

Exosomes delivering miR-129-5p combined with sorafenib ameliorate hepatocellular carcinoma progression via the KCTD1/HIF-1α/VEGF pathway

Xinyu Zhu[1,2] · Zhiwei Li[1,2] · Li Chen[1] · Limin Li[3] · Mi Ouyang[1,2] · Hao Zhou[1,2] · Kai Xiao[4] · Ling Lin[5] · Paul K. Chu[6] · Chang Zhou[1] · Chengfeng Xun[1] · Liu Yang[1] · Wenhuan Huang[1] · Xiaofeng Ding[1,2]

Accepted: 31 January 2025 / Published online: 14 April 2025

Abstract

Background Potassium channel tetramerization domain-containing 1 (KCTD1) plays a critical role in transcriptional regula-

Methods Immunohistochemistry, Western blotting and quantitative real-time PCR analysis were performed to assess the expression of KCTD1 and related genes in HCC cells. MTT assays, colony formation, cell migration, invasion and the in-vivo mouse models were utilized to evaluate the function of KCTD1 in HCC progression. Co-immunoprecipitation, chromatin immunoprecipitation and luciferase reporter assays were conducted to elucidate the molecular mechanisms of KCTD1 in HCC.

Results KCTD1 expression was increased in human HCC tissues and closely associated with advanced tumor stages. KCTD1 overexpression enhanced growth, migration, and invasion of Huh7 and HepG2 cells both in vitro and in vivo, while KCTD1 knockdown reversed these in MHCC97H cells. Mechanistically, KCTD1 interacted with hypoxia-inducible factor 1 alpha (HIF-1α) and enhanced HIF-1α protein stability with the inhibited prolyl-hydroxylases (PHD)/Von Hippel-Lindau (VHL) pathway, consequently activating the Vascular Endothelial Growth Factor (VEGF)/VEGFR2 pathway in HCC cells. Sorafenib and KCTD1 knockdown synergistically inhibited intrahepatic tumor growth following in situ injection of MHCC97H cells. miR-129-5p downregulated KCTD1 by binding to KCTD1 3′UTR. Finally, 45 μg exosomes from miR-129-5p-overexpressing MHCC97H cells combined with 25 mg/kg sorafenib to decrease HCC tumor size.

Conclusions These results suggested that KCTD1 protects HIF-1α from degradation and activates the VEGF signaling cascade to enhance HCC progression. Therefore, KCTD1 may serve as a novel target of HCC and pave the way for an combined therapy in advanced HCC.

Keywords KCTD1 · Hepatocellular carcinoma · HIF-1α · Sorafenib · Exosome

Xinyu Zhu, Zhiwei Li and Li Chen contributed equally.

✉ Limin Li
hncslilimin@hunnu.edu.cn

✉ Xiaofeng Ding
dingxiaofeng@hunnu.edu.cn

[1] The National & Local Joint Engineering Laboratory of Animal Peptide Drug Development, College of Life Science, Hunan Normal University, Lushan Road No. 14, Changsha 410081, China

[2] Key Laboratory of Model Animals and Stem Cell Biology in Hunan Province, School of Medicine, Hunan Normal University, Changsha 410013, China

[3] College of Engineering and Design, Hunan Normal University, Taozihu Road No. 68, Changsha 410081, China

[4] Department of Neurosurgery, Xiangya Hospital of Central South University, Changsha, Hunan 410008, China

[5] Department of Hepatobiliary and Pancreatic Surgery, Xiangya Hospital of Central South University, Changsha, Hunan 410008, China

[6] Department of Physics, Department of Materials Science and Engineering, and Department of Biomedical Engineering, City University of Hong Kong, Tat Chee Avenue, Kowloon, Hong Kong, China

1 Introduction

The development, progression and metastasis of hepatocellular cancer (HCC) is very devastating, and advanced HCC has an extremely poor prognosis [1, 2]. The kinase inhibitor sorafenib exhibits antiproliferative and antiangiogenic properties predominantly through inhibition of Raf-kinase and VEGFR2 and functions as one of the few FDA-approved targeted drugs to improve the median overall survival time by less than three months for patients with advanced HCC [3]. Therefore, the molecular events underlying HCC progression and improved sorafenib sensitivity need to be urgently addressed in order to develop more powerful, life-prolonging approaches for future therapeutic interventions of advanced HCC.

The BTB (Broad-Complex, Tramtrack and Bric a brac)/POZ (poxvirus and zinc domain-containing protein KCTD1 has been as a transcriptional suppressor and interacts with activator protein-2 (AP-2) transcription factor family to inhibit AP-2 transcriptional activities [4, 5]. The physiological of KCTD1 has been elucidated, KCTD1 promotes adipogenesis *via* interactions with AP-2α, a known inhibitor of adipogenesis [6]. The AP-2β/KCTD1 axis blocks renal by suppressing β-catenin activity, while KCTD1 knockout exhibits enhanced renal [7]. Although limited roles of KCTD1 have been investigated to date, these indicate that KCTD1 is associated with key transcription factors and regulates canonical signaling pathways in development, lipid metabolism and diseases.

Carcinogenesis is a complicated process involving transformation, proliferation, migration, metastasis, angiogenesis, glycolysis and immune evasion, during which multiple genes function and interact [8]. Extracellular vesicles exosomes including proteins and noncoding RNAs are key players in cancers and exerts therapeutic potential as precision medicine [9, 10]. Noncoding RNAs play a major role in not only fundamental biological processes but various human disease, especially cancer [11]. However, there is no reported evidence showing the underlying roles and mechanisms of KCTD1 in carcinogenesis. Here, the importance of KCTD1 in HCC progression is studied to the upregulation of KCTD1 expression in human HCC tissues. The tumor-promoting of KCTD1 were exerted by enhancing the HIF-1α/VEGF signaling pathway, which was reversed by the tumor suppressive gene miR-129-5p targeting KCTD1 3′UTR. KCTD1 downregulation sensitized HCC cells to sorafenib and combination therapy could inhibit HCC development by the exosome-based delivery. Our results demonstrated that the KCTD1 protein directly interacts with HIF-1α to activate the VEGF signaling cascade, thus highlighting KCTD1 as a potential clinical marker in HCC patients and novel target of HCC therapy.

2 Materials and methods

2.1 Human tissues

70 HCCs and 10 adjacent normal liver tissues were analyzed (Supplemental Tables 1, 2). The experiments were approved by Hunan Normal University in China and informed consent was gotten from all participants. IHC analysis was carried out on samples as described [12]. The protein levels of KCTD1, Ki67, CD31 and Arg1 were detected with the rabbit polyclonal antibodies against KCTD1 (bs16924R, Bioss), Ki67 (A11390, Abclonal), CD31 (ab28364, Abcam) and Arg1 (A1847, Abclonal) at 1:200 dilution followed by Maxvision^{TM}3 HRP-Polymer (Mouse/Rabbit) IHC detection Kit (KIT-5220, Maxim Biotech). The percentage of stained HCC cells was scored as follows: 0 for no staining, 1 for 1–30%, 2 for 31–60%, and 3 for 61–100%. Correlation of KCTD1 RNA expression and the overall survival of HCC patients in the TCGA cohort was analyzed by online Kaplan-Meier Plotter [13].

2.2 Cell lines

The authenticated HEK293, 293T, HCC cell lines MHCC97H, HepG2, Huh7 and Hep3B (ATCC, Manassas, USA) were cultured in DMEM medium (Hyclone, Logan, UT, USA) containing 10% fetal calf serum (FCS, Hyclone) and 1% PS antibiotics (Penicillin and Streptomycin) (Gibco). The cells were cultured at 37 °C in a 5% CO_2 .

2.3 Plasmid construction

The recombinant plasmid pCMV-Myc-KCTD1 was reported [4]. The KCTD1 cDNA was ligated into the lentiviral vector pEZ-Lv105-Puromycin (GeneCopoeia) [14]. The KCTD1 shRNA and stem-loop sequence of miR-129-5p was ligated into the GV248 vector (Genepharma, Shanghai, China). The 3′ untranslated region (UTR) fragments of the KCTD1 gene were from HEK293 genomic DNA, and ligated into the pmirGLO vector (Promega, Madison, WI, USA) between PmeI and XhoI sites. Mutagenesis of the KCTD1 3′ UTR luciferase construct was directly ligated to the pmirGLO vector to mutate the potential miR-129-5p-binding site. The mimics of miR-16-5p and miR-129-5p were synthesized by GenePharma. All the constructs had been sequenced by the sanger method for (Sangon Biotech, Co., Ltd).

2.4 Generation of KCTD1 overexpressing/knockdown and miR-129-5p overexpressing lentivirus

Lentiviral particles were generated as previously reported [12]. , 293T cells were cotransfected with the lentivirus plasmids for KCTD1 overexpression and Lenti-Pac™ HIV packaging mix (HPK-LvTR-20). The supernatants were collected, and concentrated. The Huh7, and HepG2 cells were infected with KCTD1-lentivirus [multiplicity of infection (MOI) of 5–20], 5 μg/mL polybrene (Sigma). Cells were observed under the microscope on Day 4 followed by stable cell selection with 3 μg/mL of puromycin.

The sequence of KCTD1 shRNA and pre-miR-129-5p were ligated to the lentiviral vector GV248. Recombinant vectors were cotransfected into 293T cells with pHelper1.0 and pHelper2.0 (Genepharma). The viral-containing supernatants were collected 48 h after transfection and
The MHCC97H cells were infected with lentivirus carrying KCTD1 shRNA or NC shRNA at an MOI of 10 and 5 μg of polybrene/mL, the miR-129-5p-infected MHCC97H cells were then screened with 3 μg/mL of puromycin on Day 4. The miR-129-5p-overexpressing MHCC97H cells were infected with KCTD1-overexpressing lentivirus. Mock refers to the parental cell line without any treatment.

2.5 Growth assays

For MTT analysis, 2,000 HCC cells were plated on 48-well plates either untreated or treated with sorafenib (5–10 μM) for 6 h. The cell viability at the indicated timepoints was measured with 3-(4,5-dimethylthiazol-2-yl)-2,5-diphenytetrazolium bromide solution (1 mg/mL MTT, Sigma) for 4 h at 37ºC. 100 μL of dimethylsulfoxide (DMSO) was employed to dissolve the formed formazan crystals and the absorbance of the mixture was determined using EnSpire Multimode Plate Reader (PerkinElmer, USA). Liquid colony formation assays were carried out as reported [12, 14]. 500-1,000 HCC cells were plated in duplicate on 6-well plates and cultured for 7–15 days. The cell colonies were stained for counting. All the experiments were performed in triplicate.

2.6 Migration and invasion assays

The HCC cell migration and invasion analysis was carried out as stated previously [15]. 2×10^4 of HCC cells in serum-free medium were added to the upper compartments of chambers with or without matrigel. DMEM medium with 15% FCS was put in the lower compartments. After a 24–48 h incubation period, HCC cells were and stained. The mean number of HCC cells per was calculated. These experiments were done in triplicate.

2.7 Quantitative real-time PCR

The total RNA from the HCC cell lines, and mouse and human tumor tissues were collected using the TRIzol reagent (Invitrogen, Waltham, USA) and cDNA was obtained by reverse transcription (Roche Diagnostics, Germany). qRT-PCR was performed using the SYBR Green (TakaRa, Shiga, Japan) on the Applied Biosystems 7900HT system (Weiterstadt, Germany). Reactions were performed in 384-well PCR plates following the standard qualitative PCR conditions. The forward and reverse primers are shown in Supplemental Table 3. The Ct values were detected in the exponential phase of the and the relative expression level was calculated by the ΔΔCt method compared to a reference gene.

2.8 Luciferase reporter assays

The HEK293 cells were seeded on 12-well plates and transiently cotransfected with the reporter plasmids and miRNA mimics using Lipofectamine 3000 as reported previously [16, 17]. At 24–48 h after transfection, both luciferase activities of the cellular lysate were measured using a Dual-Luciferase Assay kit (Promega). The experiments were done in triplicate.

2.9 Western blotting

The HCC cells were lysed in the RIPA lysis as reported [18, 19] and Western blots were carried out following the standard protocol. The information about the antibodies is shown in the following: rabbit polyclonal antibodies against KCTD1 (PA5-24877, ThermoFisher), AKT (A11027, Abclonal), phosphorylated AKT^{S473} (AP0140, Abclonal), HIF1α (A7684, Abclonal), ARNT (A0972, Abclonal), CD31 (A11525, Abclonal), VEGFR2 (A5609, Abclonal), p-VEGFR2 (AP0595, Abclonal), AFP (A0200, Abclonal), PHD2 (A14557, Abclonal), PHD3 (A8001, Abclonal), VHL (A0377, Abclonal), GPC3 (A12383, Abclonal) and CANX (A4846, Abclonal), rabbit monoclonal antibodies against PHD1 (A3730, Abclonal), mouse monoclonal antibodies against VEGF (A17877, Abclonal), GAPDH (AC002, Abclonal), TSG101 (16293, UpingBio), HSP70 (04337, UpingBio), CD63 (10628D, ThermoFisher) and CD81 (10630D, ThermoFisher), secondary HRP-conjugated antibodies against goat anti-rabbit (sc-2004) and anti-mouse (sc-2005) IgG (Santa Cruz Biotechnology). For protein degradation, the HCC cells overexpressing or knocking down KCTD1 were treated with cycloheximide

(CHX) at time points and concentrations and then lysed in RIPA . The HCC cells were treated with the concentration of cobalt chloride ($CoCl_2$) for 24 h to induce hypoxia, harvested and analyzed by Western blotting.

2.10 CO-IP assays

The MHCC97H cells were collected and lysed as reported [20]. The cellular extracts were immune-precipitated using polyclonal antibodies against KCTD1, ARNT or HIF-1α and protein A/G plus-agarose (Santa Cruz Biotech). The mixture was detected with rabbit anti-KCTD1 polyclonal antibodies and mouse monoclonal antibodies against HIF-1α (3C144), or ARNT (G-3, Santa Cruz Biotech). Normal rabbit IgG (sc-2027) served as the negative control.

2.11 ChIP assays

ChIP was performed using an EZ-ChIP assay kit from Upstate Biotechnology (Lake Placid, NY, USA) following the standard protocol. , 2×10^7 cells were used for further analysis. The cellular extracts were immunoprecipitated with rabbit polyclonal antibodies against KCTD1 and HIF-1α. The DNA fragments of the VEGF regulatory regions span nucleotides −1041 to -750. PCR assays were carried out using PCR primers (Supplemental Table 3).

2.12 FACS

The HCC cells were trypsinized, centrifuged and resuspended in Annexin V Binding . Cells were then labeled with both Annexin V-FITC (1 μg/mL) and propidium iodide (PI, 40 μg/mL) for 20 min in darkness at room temperature. The samples were run by BD FACSCalibur (CA, USA) and analyzed with the FlowJo 10 software.

2.13 In vivo mouse experiments

The mouse experiments were performed following the ethical principles and guidelines for Experiments on Animals and approved by Hunan Normal University. The tumorigenic capacity in vivo was determined using the xenograft mouse model. Lentivirus-infected Huh7 (1×10^7), and MHCC97H (8×10^6) were suspended in 0.2 mL of DMEM and subcutaneously injected into two points of the back of BALb/c nude mice (4-week old, female, $n = 5$ mice per group). The mice were examined every other day and the formed tumors were calculated as stated previously [21]. After two to four weeks, the mice were and subcutaneous tumors were removed, photographed and measured.

The metastatic ability in vivo was determined after intravenous injection of 5×10^6 Huh7 and MHCC97H cells into the tail veins of nude mice (6-week old, $n = 5$ per group) in two groups. The mice were after 5–6 weeks and the number of formed metastasis nodules on the surfaces of mouse lungs and livers were assessed. The lungs and livers were removed, and embedded in for further hematoxylin and eosin (HE) staining and IHC analysis.

In the mouse intrahepatic experiments, the mice in four groups with 3–4 mice in each group were administered by intrahepatic injections of 2×10^6 MHCC97H cells infected with KCTD1 shRNA. 7 days post injection, the mice were orally gavaged with 25 mg/kg of sorafenib every 2 days for 15 days or injected three times with 15 μg of exosomes per injection *via* the tail vein for two weeks. After 3 weeks, the mice were then and the livers were removed, tumor foci were photographed.

2.14 Exosome extraction

Exosomes from the cell media were extracted using an exosome isolation kit (Invitrogen, Waltham, USA) following the manufacturer's instructions. , the fresh cell medium was harvested from 8×10^6 MHCC97H cells in a volume of 15 mL culture medium and cells were grown without FBS for 24 h. The culture medium was centrifuged at 700 × g for 8 min to remove the cells and debris. Then, the medium was through 0.22-μm-pore-size nitrocellulose membrane, the supernatant was added to 7.5 mL of total exosome isolation reagent and the samples were mixed and incubated overnight at 4 °C. Then, samples were centrifuged at 13,000 × g at 4 °C for 70 min. The pellet was resuspended and washed followed by 100,000 × g centrifugation for 90 min. The pelleted exosomes were dissolved in 80 μL of PBS and stored at -80 °C. By dropping the exosome suspensions onto an electron microscopy copper grid, the morphology of exosomes was determined by transmission electron microscopy (TEM, JEOL2100, Japan).

2.15 Statistical analysis

The data analysis was performed using SPSS 16.0 software (Chicago, IL, USA) and Prism 6 statistical software (San Diego, CA, USA) and the Pearson's $\chi 2$ test was applied to evaluate the association between gene expression and clinical parameters. The expression levels of interest genes between HCC tissues and non-tumor tissues were assessed with Student's *t*-test. The two-way ANOVA was performed to compare more than two groups. Multiple comparisons among groups were carried out using the Tukey's test in the post-hoc analysis. The survival function was estimated by the Kaplan-Meier curve. All data are presented as

the mean ± SD of at least three independent experiments and *P*

3 Results

3.1 KCTD1 upregulation in HCC tissues

To measure the clinical of KCTD1 in malignant tumors, the expression level of KCTD1 in 10 normal livers and 70 HCCs was detected by IHC analysis. KCTD1 was highly expressed in 50% of adjacent normal liver tissues and detected in 10 (14%) of the 70 HCCs as indicated by intense staining (3+). 23 (33%) of the 70 HCCs were moderately positive (2+) and 37 (53%) were weakly positive or negative for KCTD1 expression (1+/0) (Fig. 1A, B). Clinicopathologic association analysis of the HCCs revealed that KCTD1 expression is associated with the advanced clinical stage of HCC (Supplemental Table 1). Low KCTD1 expression was observed from low-grade hepatocellular cancers (I/II), whereas high KCTD1 expression was detected from high-grade HCC (III/IV) ($P < 0.05$) (Fig. 1B). In paired HCC and adjacent non-tumor samples, KCTD1 expression showed a high proportion of upregulation in the HCC samples compared with non-tumor samples as analyzed by quantitative RT-PCR and Western blots (Fig. 1C, D). Furthermore, high-level KCTD1 expression was correlated negatively with the overall survival of patients according to Kaplan-Meier Plotter database (Fig. 1E) and therefore, KCTD1 expression increased in high-grade HCC tissues.

3.2 KCTD1 overexpression enhances both in vitro and in vivo proliferation, migration and metastasis of HCC cells

The of KCTD1 overexpression on the malignancy of human HCC were analyzed by examining the expression of the KCTD1 protein in the HCC cell lines. The relatively low expression of KCTD1 proteins was detected in human hepatoma cell lines HepG2, Hep3B, and Huh7, while high expression of KCTD1 was found from MHCC97H cells (Supplemental Fig. 1A). To evaluate the role of KCTD1 in HCC, stable expression HCC cell lines (pFLAG-KCTD1 and pFLAG-NC) were generated with HepG2 and Huh7 cells (Supplemental Fig. 1B). Western blotting demonstrated overexpression of KCTD1 in both HCC cell lines (Fig. 2A). KCTD1 overexpression resulted in more viable HCC cells (Supplemental Fig. 1C), increased colony number, and larger HCC cell size than the control cells (Fig. 2B and Supplemental Fig. 1D), indicating the strong tumorigenicity of KCTD1. Transwell cell migration and invasion assays indicated that overexpression of KCTD1 results in a increase in the HCC cell motility (Supplemental Fig. 1E), and more KCTD1-overexpressing HCC cells than control cells are invasive (Supplemental Fig. 1F). These results suggested that KCTD1 increases the in vitro proliferation, migration, and invasion of HCC cells.

To corroborate the similar of KCTD1 overexpression on the tumorigenic ability of HCC cells in vivo, KCTD1 LV-infected Huh7 cells were injected subcutaneously into the back of female nude mice. Within 4 weeks, the mean tumor weight and volume in the KCTD1 group increased in comparison with the control group mice (Fig. 2C-E). HE staining that the HCC cells are arranged tightly in the KCTD1 group (Fig. 2F) and IHC staining showed that KCTD1 overexpression increases the expression of the proliferation marker Ki67 in the subcutaneous tissues derived from Huh7 cells (Fig. 2G, H). These indicated that KCTD1 overexpression enhances the tumorigenic ability of HCC cells in vivo.

KCTD1 overexpressing Huh7 cells and control cells were injected into the tail veins of female nude mice to check for the lung metastasis, the metastatic nodules were visible on the surfaces of lungs but not livers examined after six weeks (Fig. 2I). HE staining revealed that the mice from the KCTD1 group have larger lung metastatic nodules, while a few smaller nodules are detected from mice with control cells. Metastatic nodules also appeared from mouse liver tissues obtained from the KCTD1 group (Fig. 2J). These demonstrated that KCTD1 overexpression promotes the in vivo invasion and metastasis of HCC cells.

3.3 KCTD1 knockdown suppresses the in vitro and in vivo proliferation, migration and metastasis of HCC cells

To the role of KCTD1 in human HCC, the stable cell lines (GFP-KCTD1 shRNA and GFP-NC shRNA) were established in MHCC97H cells (Supplemental Fig. 2A). Western blotting demonstrated knockdown of KCTD1 expression in HCC cell lines (Fig. 3A). KCTD1 knockdown decreased the HCC viable cell number (Supplemental Fig. 2B) and suppressed the number and size of HCC cell colonies (Fig. 3B and Supplemental Fig. 2C). Transwell migration and invasion assays disclosed that knocking down KCTD1 results in a decrease in the cell motility (Supplemental Fig. 2D, E) and a fewer number of HCC cells with KCTD1 knock down invade through the matrigel-coated chamber compared to the number of control HCC cells (Supplemental Fig. 2F, G). The data showed a strong antitumorigenic role for KCTD1 downregulation.

The of KCTD1 knockdown on the tumorigenicity of HCC cells was examined in vivo. MHCC97H cells stably infected with KCTD1 shRNA-LV or control NC-LV

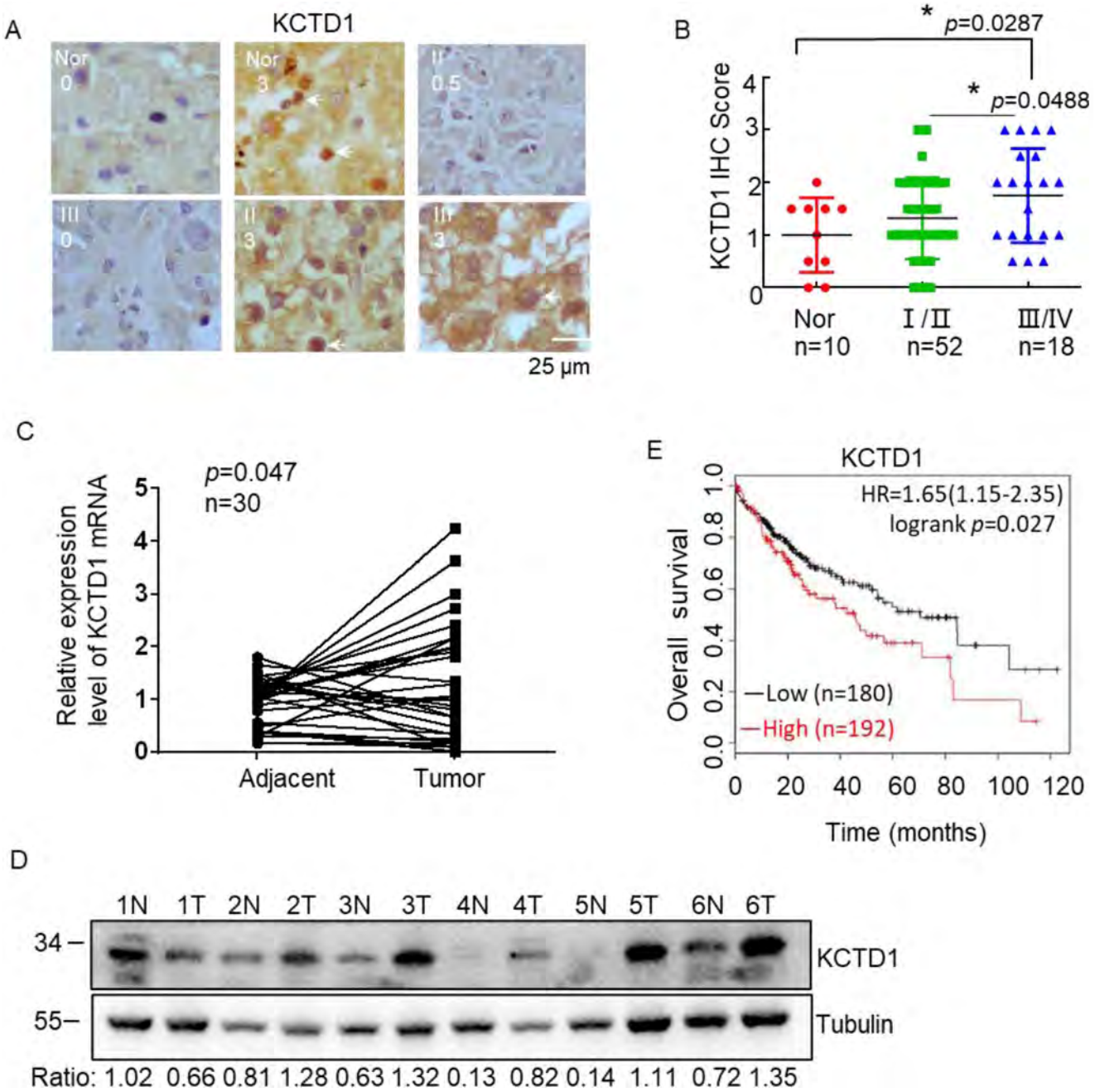

Fig. 1 Expression levels of KCTD1 in HCC tissues. **A** KCTD1 expression detected by IHC staining in 70 HCCs and 10 normal liver tissues. Arrowheads indicate positive staining. I, II, III, IV, degrees of pathological staging; Nor, normal. **B** IHC score of HCCs and adjacent normal liver tissues detected with the polyclonal anti-KCTD1 antibodies. The staining intensities are scored as 0–3 and each symbol indicates an individual case. *, $p<0.05$. **C**, **D** KCTD1 mRNA and protein levels in paired hepatocellular cancer tissue samples detected by qRT-PCR and Western blots. N, normal; T, tumor. **E** Correlation of KCTD1 mRNA expression and the overall survival of HCC patients in the TCGA cohort

s.c. were injected into the back of nude mice, individually and after 2 weeks, the mean tumor weight and volume of the KCTD1-knockdown group decreased compared with the NC group (Fig. 3C-E). HE staining that the MHCC97H cells are arranged loosely in the KCTD1 shRNA group (Supplemental Fig. 2H) and IHC analysis showed that KCTD1 knockdown inhibits the expression of Ki67 (Fig. 3F, Supplemental Fig. 2I). KCTD1 shRNA cells and control MHCC97H cells were intravenously injected via the tail vein into female nude mice and after six weeks, the metastatic nodules were calculated on the surfaces of mouse lungs not livers (Fig. 3G, Supplemental Fig. 2J). The

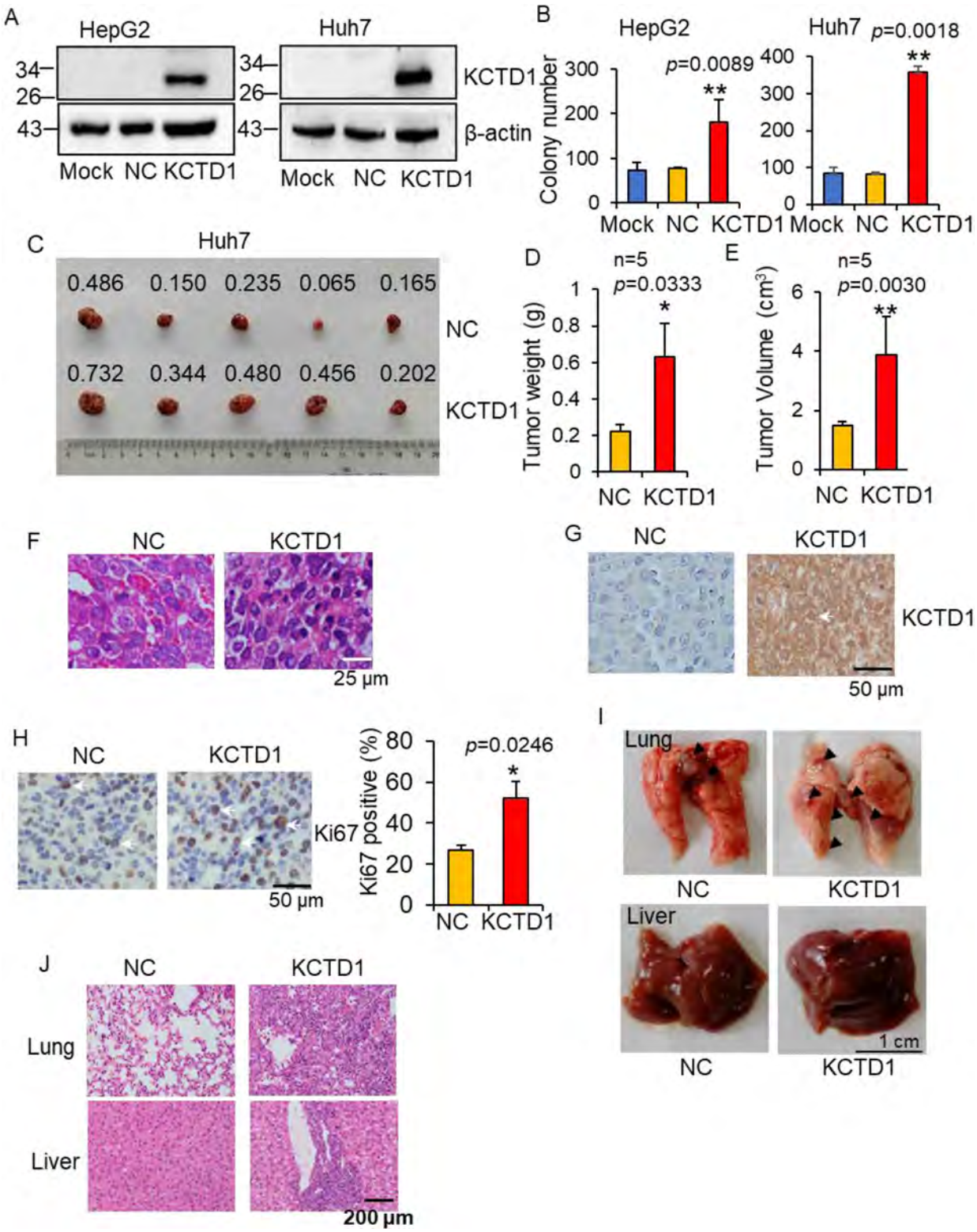

Fig. 2 of KCTD1 overexpression on the in vitro and in vivo growth and migration of HCC cells. **A** Western blotting of KCTD1 expression in HCC cell lines. **B** Liquid colony formation assay of both HCC cell lines infected with KCTD1-LV. **C-E** Approximately 1×10^7 infected Huh7 cells injected subcutaneously into the back of immunonude mice (female, $n = 5$/group). After 4 weeks, the subcutaneous tumors were removed, weighed and measured. **F** HE staining carried out on serial 5 μm sections of subcutaneous tumors derived from Huh7 cells. **G** IHC staining of KCTD1 expression in Huh7 tumors. **H** IHC staining of Ki67 expression in Huh7 tumors and of Ki67-positive cells shown. Arrowheads indicate positive staining. **I** Pictures of metastatic lungs and livers of female nude mice through tail vein injection of Huh7 cells. **J** Representative HE staining carried out on mouse lung and liver tissues six weeks after tail-vein injection with Huh7 cells. *, $p < 0.05$ and **, $p < 0.01$

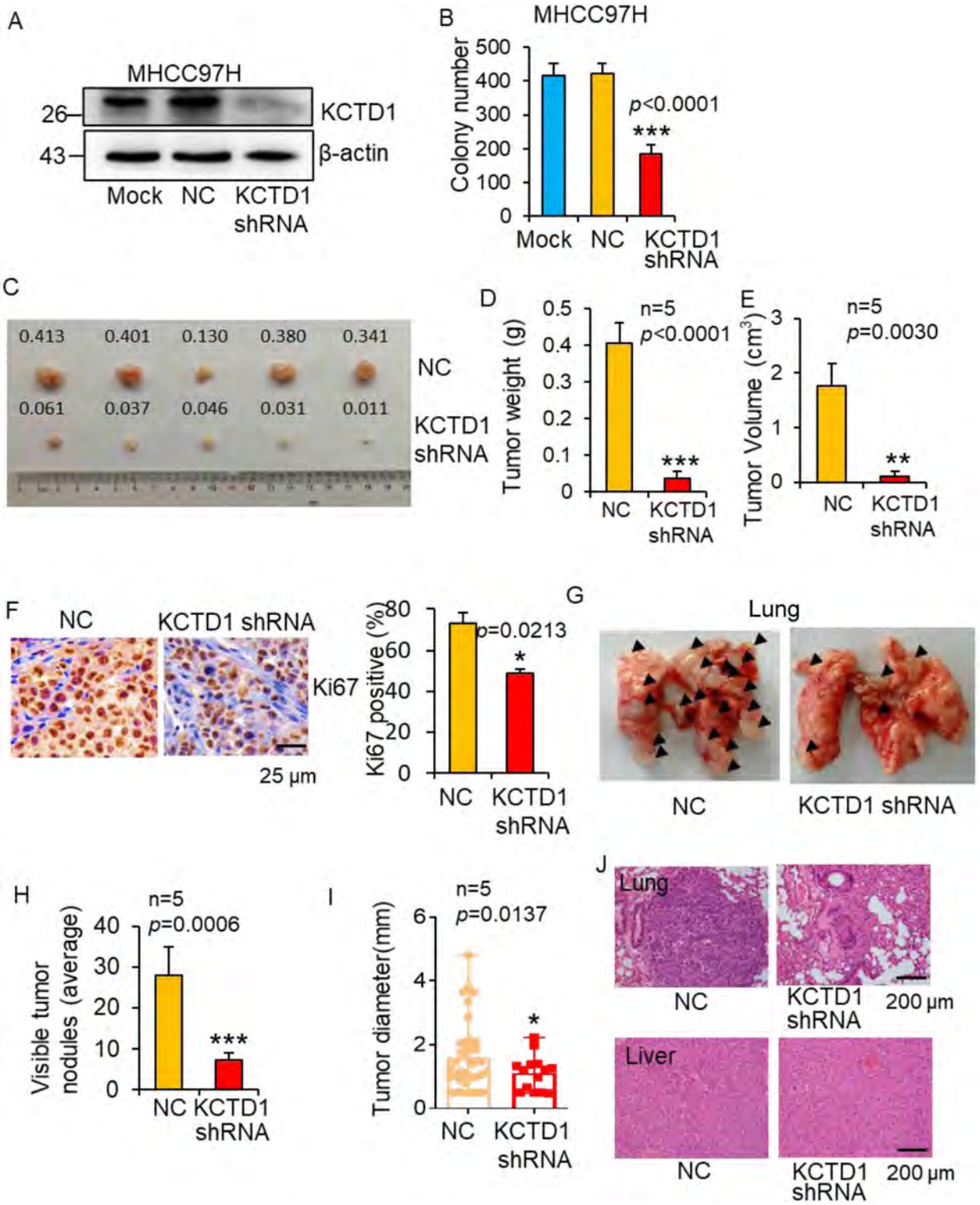

Fig. 3 of KCTD1 knockdown on HCC growth and migration in vitro and in vivo. **A** Western blotting of KCTD1 expression in NC shRNA- and KCTD1 shRNA-infected MHCC97H cells. **B** Liquid colony formation assays of infected HCC cells. **C-E** About 8×10^6 infected MHCC97H cells injected subcutaneously into the two points of the back of nude mice (4-week old, female, $n=5$/group). After 15 days, the tumors were removed and measured. **F** IHC staining of Ki67 expression in MHCC97H tumors and of Ki67-positive cells shown. Arrowheads indicate positive staining. **G-I** The average number and diameter of lung nodules from nude mice were six weeks after intravenous injection of MHCC97H cells ($n=5$ per group). **J** HE staining carried out on the lung and liver tissues after tail-vein injection. *, $p<0.05$, **, $p<0.01$, and ***, $p<0.001$

mice in the KCTD1 shRNA group had increasingly fewer and smaller lung metastatic nodules than those in the NC shRNA group (Fig. 3H, I). Tumor foci in mouse lungs were detected by HE staining, while the liver morphology did not change obviously in the two groups of mice (Fig. 3J). Altogether, these results demonstrated that KCTD1 downregulation suppresses HCC cell proliferation, migration, and metastasis in vivo, suggesting that KCTD1 knockdown markedly suppresses the tumorigenic ability of HCC cells.

3.4 KCTD1 activates the HIF-1α/VEGF pathway by interacting with HIF-1α

HIF-1α mediates the hypoxia-induced expression of VEGF, which plays a central role in angiogenesis and tumor progression [22]. The single cell RNA sequencing data showed KCTD1 is expressed in endothelial cells of HCC (Supplemental Fig. 3A). TCGA data analysis showed that KCTD1 expression positively correlates with VEGF expression (Supplemental Fig. 3B). A stable HUVEC line that overexpressed KCTD1 protein was then generated (Supplemental Fig. 3C) and it is found that KCTD1 enhances proliferation of HUVECs in vitro (Supplemental Fig. 3D). KCTD1 overexpression induced HUVEC tube formation and increased the branch counts of formed tubes and the number of HUVEC-formed tubes (Supplemental Fig. 3E). Moreover, KCTD1 overexpression improved phosphorylation of VEGFR2 and promoted the expression of VEGF, HIF-1α and ARNT in HUVECs (Supplemental Fig. 3F). These indicated that KCTD1 overexpression promotes the angiogenesis through activating the VEGF signaling cascade in vitro. Next, we wonder whether KCTD1 regulates the HIF-1α/VEGF pathway in HCC cells. KCTD1 overexpression promoted the expression of the p-VEGFR2/p-AKT/ HIF-1α-ARNT/VEGF cascade in Huh7 cells (Fig. 4A), while KCTD1 knockdown decreased the expression of these proteins in MHCC97H cells (Fig. 4B). Notably, KCTD1 the expression of HCC clinical biomarkers GPC3 and AFP [23, 24]. Decreased levels of ARNT and HIF-1α were observed in the KCTD1 shRNA group from the mouse subcutaneous tumor tissues (Supplemental Fig. 4A). The KCTD1 protein stability assays showed that an increasing amount of HIF-1α proteins is measured from the KCTD1 overexpressing Huh7 cells treated with CHX (Supplemental Fig. 4B). In contrast, more decrease in HIF-1α/ARNT proteins was induced in the KCTD1-knockdown MHCC97H cells than in the control cells treated with different concentrations of CHX at time points (Supplemental Fig. 4C, D). $CoCl_2$ induces the expression of HIF-1α in the HCC cells [25]. KCTD1 overexpression led to increased HIF-1α proteins in Huh7 cells (Supplemental Fig. 4E), but KCTD1 knockdown resulted in decreased HIF-1α proteins in MHCC97H cells (Supplemental Fig. 4F). HIF-1α underlies oxygen dependent degradation whereas ARNT expression is constant [26], which is consistent with our results (Supplemental Fig. 4G). Simultaneously, hypoxia prevented the degradation of KCTD1. In normoxia, the hydroxylated HIF-1α is targeted for degradation by the pVHL E3 ubiquitin ligase complex [27]. KCTD1 overexpression enhanced HIF-1α stability with decreased PHD2, PHD3 and pVHL (Fig. 4C), whereas KCTD1 knockdown inhibited the expression of HIF-1α with improved PHD2, PHD3 and pVHL (Fig. 4D), indicating the of KCTD1 on HIF-1α stability in a PHD/VHL dependent manner. The expression of Arg1 is increased in HIF-1α–positive myeloid-derived suppressor cells (MDSC) [28]. IHC staining showed that KCTD1 knockdown reduces the expression of Arg1 and vice versa (Fig. 4E, Supplemental Table 4). These data suggested that KCTD1 regulates the stability of heterodimer HIF-1α/ARNT proteins.

To further disclose the regulatory relationship of KCTD1 and HIF-1α/ARNT genes, co-immunoprecipitation assays were carried out. Endogenous HIF-1α was detected from immune complexes of overexpressed KCTD1 (Fig. 4F) and endogenous ARNT could not appear from the immunoprecipitates of overexpressed KCTD1 (Fig. 4G), suggesting an interaction between KCTD1 and HIF-1α. As reported [29–31], ARNT formed a heterodimer with HIF-1α (Supplemental Fig. 4H). Hypoxia augmented the interaction between HIF-1α/KCTD1 and HIF-1α/ARNT (Fig. 4H), which may elucidate that KCTD1 changes ARNT expression by improving HIF-1α expression. Chromatin immunoprecipitation using anti-KCTD1 and anti- HIF-1α antibodies showed enrichment of VEGF promoter fragments with HIF-1α-binding sites compared to that of IgG (Fig. 4I), indicating that KCTD1 forms a complex with HIF-1α/ARNT and binds with the VEGF promoter [32]. IHC staining showed that KCTD1 overexpression elevates the expression of endothelial marker CD31 in Huh7 cells, while KCTD1 knockdown eliminates the expression of CD31 in MHCC97H cells (Supplemental Fig. 4I, Supplemental Table 5). Taken together, these data showed that KCTD1 could bind with the HIF-1α/ARNT heterodimer to regulate the VEGF signaling pathway.

3.5 Sorafenib increases the cytotoxicity of HCC cells knocking down KCTD1 both in vitro and in vivo

HCC has a poor prognosis due to its high incidence of recurrence and metastasis and postoperative chemotherapy is necessary [33]. The of KCTD1 knockdown on the chemosensitivity of HCC cells were studied. The MTT absorbance in the KCTD1-knockdown and sorafenib-treated HCC cells strikingly decreased than that in control

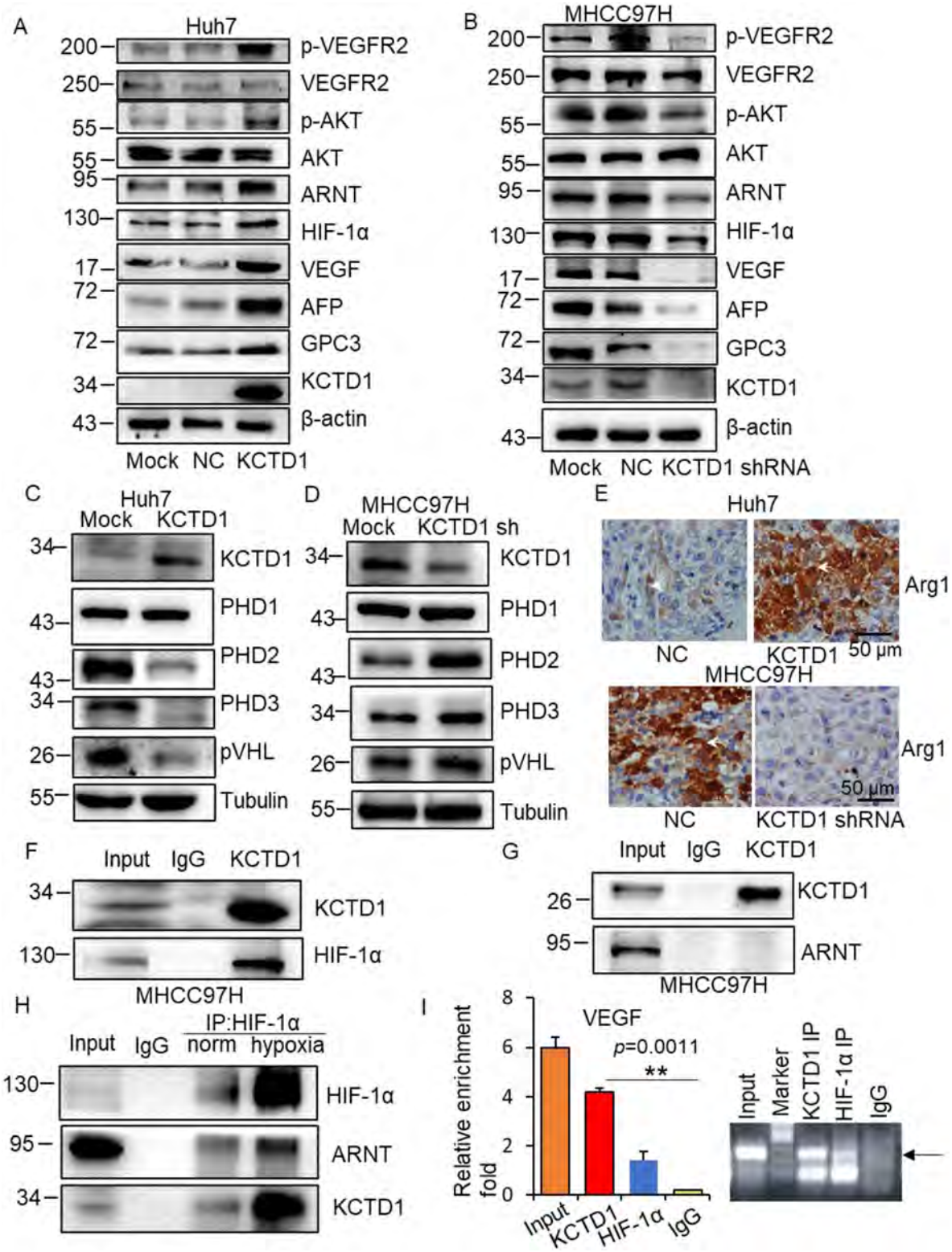

Fig. 4 Regulation mechanism of KCTD1 on the HIF-1α/VEGF signaling pathway. **A**, **B** Western blots detecting the expression change of the HIF-1α/VEGF signaling pathway in KCTD1-overexpressing Huh7 cells and KCTD1-knockdown MHCC97H cells. **C**, **D** Western blots detecting the of KCTD1 overexpression/knockdown on the stability of PHD and pVHL. **E** IHC staining of Arg1 expression in Huh7 and MHCC97H tumors. **F**, **G** Co-immunoprecipitation analysis performed to demonstrate the interaction between KCTD1 and HIF-1α, KCTD1 and ARNT using KCTD1 antibodies. **H** Co-immunoprecipitation analysis performed to detect the interaction between KCTD1/HIF-1α, and HIF-1α/ARNT in normoxic conditions and hypoxia. **I** Chromatin immunoprecipitation performed to the binding of KCTD1 and HIF-1α with the VEGF promoter. The amount of PCR products is detected on 2% agarose gels. **, $p<0.01$

cells on Day 3. And the absorbance decreased by 32% in the KCTD1-knockdown HCC cells compared to the control cells, while 69% reduction in the MTT absorbance appeared from the KCTD1-knockdown HCC cells treated with sorafenib on Day 5 (Fig. 5A), suggesting that the combination of KCTD1 knockdown with sorafenib reinforces the HCC cell cytotoxicity.

After treatment with sorafenib, cell apoptosis of the KCTD1 shRNA-infected and parental MHCC97H cells was detected by cytometry. The rate of apoptosis increased for cells with sorafenib treatment and KCTD knockdown, as independently and synergistically compared to the proportion of the control cells (Fig. 5B and Supplemental Fig. 5). The of KCTD1 downregulation and sorafenib on tumor formation in intrahepatic mouse models were probed. Both treatments resulted in smaller tumor foci in the mouse livers and a lower liver/body weight ratio than single treatment group and the control group (Fig. 5C, D). Clinically, the low expression of KCTD1 led to a prolonged median overall survival of 30.9% in 29 sorafenib-treated patients with recurrent HCC, although there was no statistical sig- (Fig. 5E). The results revealed that KCTD1 knockdown and sorafenib synergistically repress HCC progression.

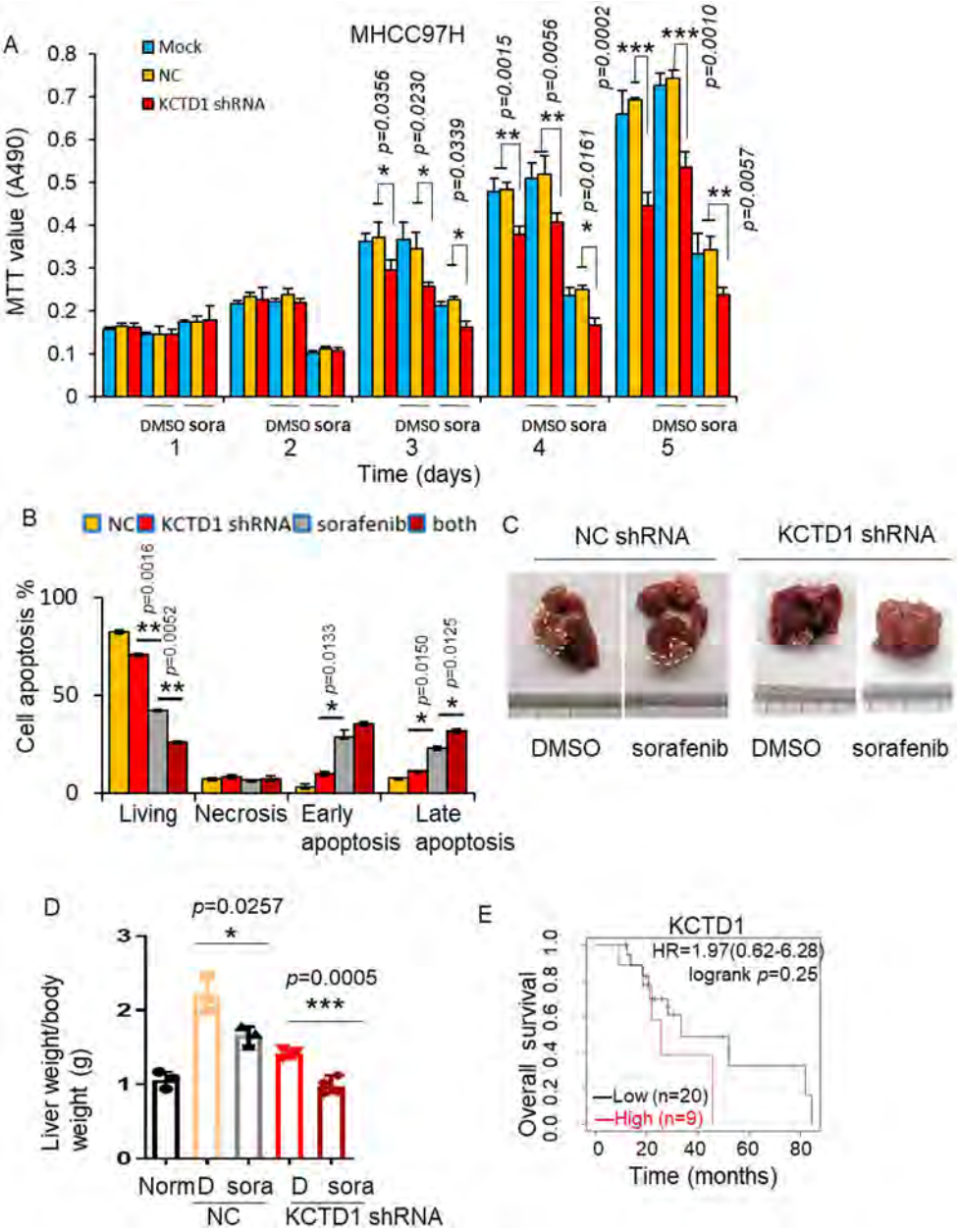

Fig. 5 KCTD1 knockdown increasing the sensitivity of HCC to sorafenib. **A** Uninfected and infected MHCC97H cells treated with 5 μM of sorafenib or control agent DMSO for 24 h and cell viability assays analyzed by MTT for 5 days. Sora, sorafenib. **B** Apoptosis assays of MHCC97H . Cells infected with KCTD1 shRNA-LV are treated with 5 μM of sorafenib or DMSO for 24 h and cellular apoptosis is detected by FACS analysis. **C**, **D** Intrahepatic tumor model generated by injecting 2×10^6 MHCC97H cells. 7 days later, the mice were orally received with the control solvent or 25 mg/kg sorafenib every other day for 2 weeks. The tumor-loaded livers and liver to body weight ratio were shown. $n = 3$ mice/group. D, DMSO; sora, sorafenib. **E** Correlation of KCTD1 expression and the overall survival of HCC patients treated with sorafenib in the TCGA cohort. Norm, uninjected normal mice; D, DMSO; sora, sorafenib

3.6 miR-129-5p targets the KCTD1 3′ UTR and decreases the tumor-promoting effects of KCTD1 in HCC in vitro as well as in vivo

Because KCTD1 downregulation suppressed HCC progression, miRNAs targeting the KCTD1 3′ UTR were predicted by TargetScan, miRWalk, RNA22 and miRanda, potential miR-129-5p and miR-16-5p binding sites were found (Fig. 6A). KCTD1 3′ UTR luciferase reporter vectors were cotransfected into HEK293 cells with miRNA mimics. The overexpression of miR-16-5p and miR-129-5p suppressed the luciferase activities of 3′ UTR of the KCTD1 gene. miR-129-5p more tly downregulated KCTD1 (Fig. 6B) and decreased the mRNA level of KCTD1 (Fig. 6C). However, miR-129-5p showed no on the luciferase activity of mutated miR-129-5p response element within seed sequences of KCTD1 (Supplemental Fig. 6A), indicating that miR-129-5p binds with KCTD1 3′UTR via miR-129-5p-binding sites. miR-129-5p overexpression could decrease the expression of KCTD1 protein as well as that of HIF-1α and ARNT proteins (Fig. 6D). KCTD1 overexpression rescued the expression of miR-129-5p-inhibited KCTD1/HIF-1α/ARNT axis (Fig. 6E). These data revealed that miR-129-5p targets the 3′ UTR region of KCTD1 gene and downregulates KCTD1 expression.

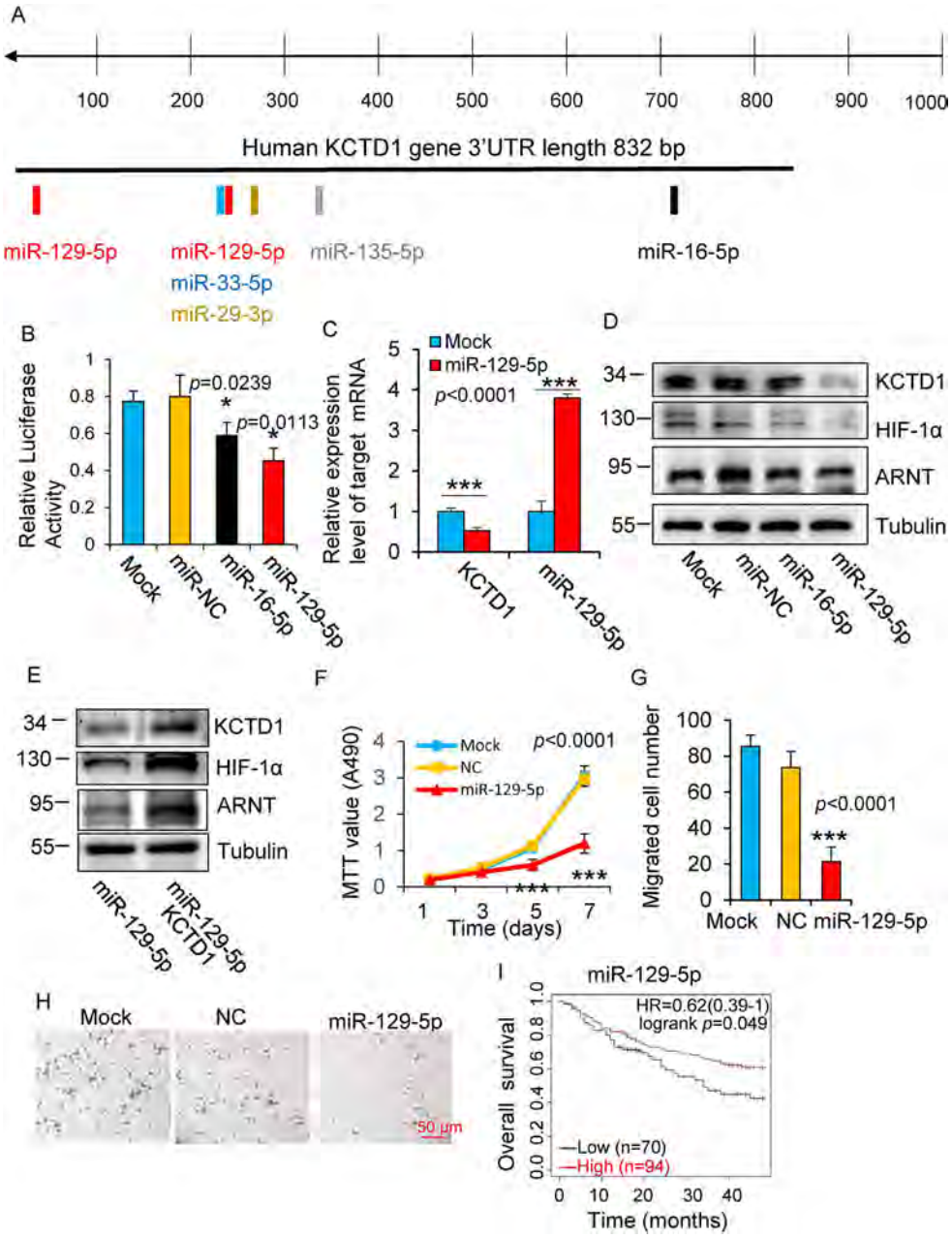

Fig. 6 miR-129-5p targeting of KCTD1 in HCC cells. **A** Possible binding sites of miRNAs in the 3′-UTR of KCTD1. **B** miR-129-5p regulating KCTD1 3′-UTR luciferase activity. is normalized to the Renilla background. **C** miR-129-5p overexpression on KCTD1 mRNA levels in MHCC97H cells. **D** Western blotting of the KCTD1 and HIF-1α/ARNT expression after miR-129-5p and miR-16-5p transfection. **E** Western blotting detecting the of miR-129-5p rescued by KCTD1 in MHCC97H cells. **F** MTT analysis of miR-129-5p infected MHCC97H cells. **G**, **H** overexpression on MHCC97H cell migration. **I** Correlation of miR-129-5p expression and the overall survival of HCC patients in the TCGA cohort

To demonstrate the critical role of miR-129-5p in KCTD1-mediated HCC cell growth, MHCC97H cells were infected with miR-129-5p LV (Supplemental Fig. 6B), miR-129-5p dramatically suppressed growth (Fig. 6F) and migration of the MHCC97H cells (Fig. 6G, H). miR-129-5p was positively linked with overall survival time of HCC patients according to TCGA database (Fig. 6I). The results indicated that the tumor inhibitor miR-129-5p decreases the tumor

3.7 Exosomes delivering miR-129-5p combine with sorafenib to suppress intrahepatic tumor growth

Exosomes can serve as cargos to deliver miRNAs to target organs conveniently and [34, 35]. Exosomes are adopted to analyze the of miR-129-5p. The morphology of exosomes was examined by TEM (Fig. 7A). Expression of exosome positive markers CD81, CD63, TSG101, HSP70 and negative marker CANX was (Fig. 7B). Expression level of miR-129-5p was markedly increased in exosomes from the supernatant of miR-129-5p-LV infected MHCC97H cells (Fig. 7C). The expression of KCTD1 and HIF-1α proteins were decreased in MHCC97H cells treated with miR-129-5p-overexpressing exosomes (Fig. 7D). miR-129-5p-overexpressing exosomes were injected into the tail veins of an intrahepatic tumor model leading to a fewer number and smaller size of tumor foci in the livers (Fig. 7E). The combination of exosomes and sorafenib treatment synergistically reduced the size and number of the tumor foci, the weight of liver tissues and downregulated KCTD1 and HIF-1α expression compared with those in the control groups (Fig. 7F-H). These results suggested that miR-129-5p-overexpressing exosomes synergize sorafenib to suppress intrahepatic tumor development, indicating the possibility of a combined therapy consisting of sorafenib and KCTD1 knockdown for treating advanced HCC.

4 Discussion

The biological importance of KCTD1 in transcription regulation, adipogenesis, and SEN disease has been studied [6, 7, 36], but the potential function of KCTD1 in malignant tumorigenesis remains unknown. In the current study, the variable level of KCTD1 expression is found in HCC tissues, but high expression of KCTD1 is detected from 47% of HCC samples, and KCTD1 expression is positively associated with tumor grade. The cell-surface marker GPC3 is expressed at high levels in HCCs and serves as a serum marker of HCC [23]. Serum alpha-fetoprotein (AFP) is used as a tumor marker for detection and diagnosis of HCC patients [24]. Overexpression of the KCTD1 protein increased the protein levels of AFP and GPC3 in HCC cell lines and simultaneous tion of KCTD1/GPC3/AFP may improve the sensitivity for diagnosis of HCC. The data thus indicate the potential clinical importance of KCTD1 in molecular clinical characteristics, and detection of HCC.

Our functional assays that KCTD1 overexpression promotes HCC cell growth, migration, and invasion of HCC cells. These malignant features are ameliorated by KCTD1 knockdown or application of its upstream regulator miR-129-5p, which targets the KCTD1 3' UTR. Murine subcutaneous and pulmonary metastasis experiments demonstrated that KCTD1 enhances the tumor formation ability and increases the number of lung tumor nodules in vivo, while KCTD1 knockdown suppresses these miR-129-5p and miR-16-5p have been reported to function in the occurrence and development of various malignant tumors [37–39] and block HCC progression [40–42]. As a negative target of Myc, miR-129-5p could block glycolysis via targeting the mitochondrial matrix protein pyruvate dehydrogenase kinase 4 (PDK4) to suppress HCC [40]. In mouse tumor models, overexpression of miR-16-5p could retard the carcinogenic process by regulating the expression of long non-coding RNAs [39]. As expected, miR-129-5p and miR-16-5p mimics downregulated KCTD1 expression and miR-129-5p exerted tumor suppressive These indicate the tumor-promoting ability of the KCTD1 protein in HCC. HIF-1α heterodimerizes with ARNT, promoting the expression of VEGF upon binding with the hypoxia-response element (HRE) in the VEGF promoter [43, 44]. VEGF is discovered in diverse cancers and stimulates vascular endothelial cell growth, and survival in the tumors [45, 46]. The VEGF ligands such as VEGF-A, Ang1/2 and their receptors including VEGFR1/2 and Tie2 are critical regulators of tumor angiogenesis and vasculogenesis pathways [47]. Some factors such as activator 1 (SP1), and HIF-1α have been found to regulate VEGF expression [48–50]. In our study, KCTD1 can enhance the stability of the HIF-1α/ARNT heterodimer, consequently activating the expression of the downstream VEGF/p-VEGFR2/p-AKT/HIF-1α signaling cascade to form a positive feedback loop (Fig. 8). In normoxic conditions, the HIF-1α proteins are with prolyl hydroxylation by PHD, which was recognized by the E3 ubiquitin ligase complex containing pVHL for the degradation of HIF-1α [27, 51, 52]. Mechanistically, KCTD1 interacted with HIF-1α to enhance HIF-1α stability and concurrent decrease in PHD2/3 and pVHL expression, while KCTD1 knockdown promoted the degradation of HIF-1α for the binding of activated PHD2/3 and pVHL, indicating the potential competition between KCTD1 and pVHL for binding to HIF-1α.

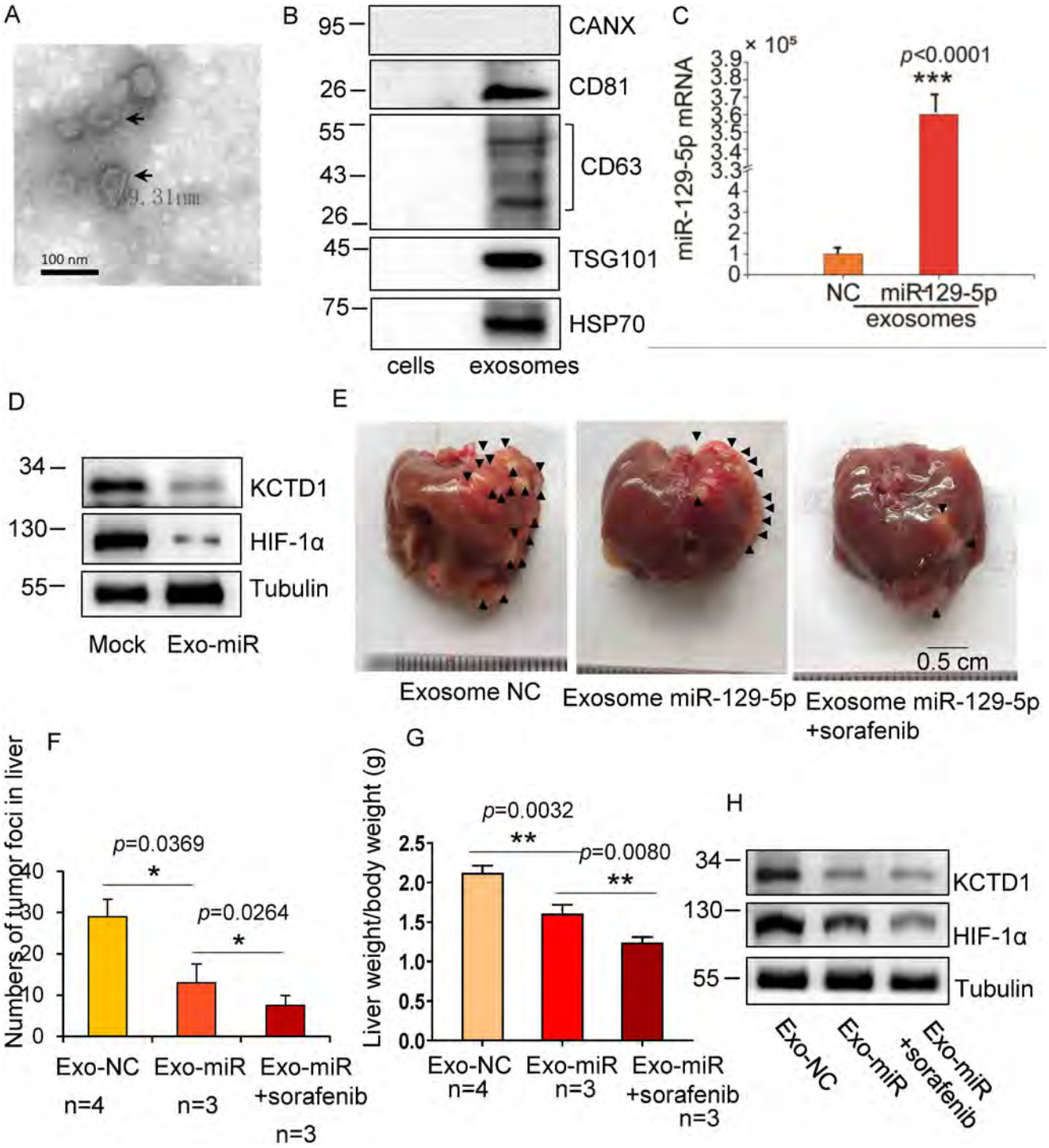

Fig. 7 Exosomes delivering miR-129-5p and sorafenib synergistically suppressing HCC tumor size. **A** Exosomes from the supernatant of MHCC97H cells extracted and detected by TEM. **B** Western blots of the expression of exosome markers. **C** qRT-PCR analysis of mRNA levels of miR-129-5p from these exosomes. **D** Western blotting of the KCTD1 and HIF-1α expression in MHCC97H cells after treatment with exosomes overexpressing miR-129-5p. **E-G** MHCC97H cells injected into the liver of nude female mice. After one week, the mice were orally treated with 25 mg/kg sorafenib every other day and 45 μg of exosomes per mouse three times for 2 weeks. The tumor-loaded livers were indicated, the tumor foci in the liver were and the ratios of tumor-loaded liver/body weight were measured. **H** The expression of KCTD1 and HIF-1α proteins in tumors was detected. $n = 3$–4 mice/group

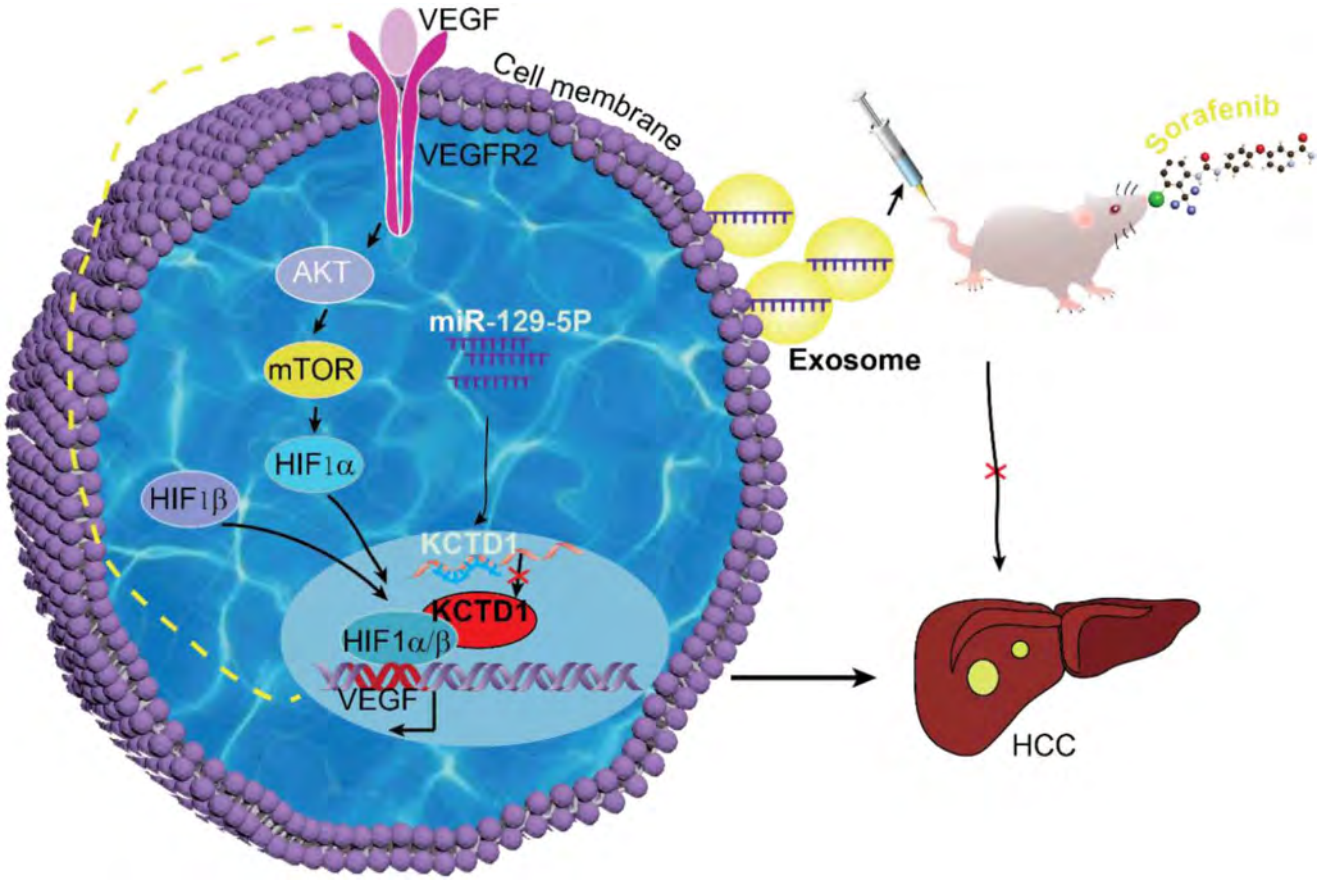

Fig. 8 Schematic representation of the possible mechanism underlying KCTD1-enhanced HCC progression. KCTD1 interacts with HIF-1α/β in the nucleus, binds with the promoter of the VEGF gene, and activates VEGF expression, subsequently binding with VEGFR2 on the HCC cell surface and promoting the VEGF caspase signal pathway. On the one hand, miR-129-5p binds with 3′UTR of the KCTD1 gene, suppresses KCTD1 protein level, and exosomes delivering miR-129-5p reverse its tumor-promoting role of KCTD1. On the other hand, sorafenib and KCTD1 knockdown synergistically inhibit HCC progression. HIF-1β designates as ARNT

And KCTD1 interacts with the transcription factor AP-2 [5], there are canonical AP-2 binding sites in the promoters of VHL and PHD2/3 genes by JASPAR database analysis, indicating that KCTD1 may indirectly HIF-1α expression through other complexes.

Tumor-associated macrophages (TAMs) are associated with tumor survival, angiogenesis and chemoresistance [53]. The M2-type macrophages promote tumor angiogenesis, invasion and metastasis of HCC [54]. M2 macrophage marker Arg1 is induced by TAMs in response to HIF/VEGF signaling [55, 56]. Arg1 increases vessel density and enhances myeloid cell adhesion [57]. And Myocardial capillary density was increased by upregulated expression of VEGF and CD31 by regulating the HIF-1α/VEGF pathway [58]. HIF-1α expression in uveal melanoma was - cantly correlated with vascular (CD31 and VEGF-A) markers [59]. The expression of CD31 and Arg1 was enhanced in KCTD1-overexpressing HCC cells, which demonstrated that KCTD1 regulates HIF-1α signaling pathway improving the levels of downstream genes VEGF, Arg1 and CD31 expression in both HCC and HUVEC cells, suggesting the potential importance of KCTD1 between angiogenesis and tumor immunity. It is interesting to elucidate the - cance and cross-interactions of KCTD1 to reveal the therapeutic implications of KCTD1 in individual HCC cases. Altogether, the data show that KCTD1 is an important regulator of the HIF-1α/VEGF pathway.

Sorafenib suppresses the RAS/RAF/MEK/ERK pathway, and blocks tumor proliferation and angiogenesis in human HCC [60]. Sorafenib robustly enhances KCTD1 knockdown-induced apoptosis of HCC cells and the synergistic is demonstrated in intrahepatic HCC mouse models, indicating that KCTD1 knockdown increases the sensitivity of HCC cells to sorafenib. Exosomes are involved in the contact between non-HCC cells and HCC cells and regulate the progression of HCC [61]. Exosomes transfer miRNAs to exhibit therapeutic for numerous tumors including HCC [9, 38]. miR-129-5p-overexpressing exosomes markedly reduced the growth of intrahepatic tumor. And miR-129-5p combined with sorafenib to dramatically suppress

the progression of HCC. These suggest a novel therapeutic strategy of combined sorafenib and KCTD1 knockdown for advanced HCC.

KCTD1 promotes proliferation and migration of HCCs by interacting with HIF-1α and activating the HIF-1α/VEGF pathway, while KCTD1 knockdown, miR-129-5p or the exosome delivery targeting KCTD1 suppress tumor development, indicating that KCTD1 exerts a tumor-promoting role in HCC. Understanding functions and mechanisms of KCTD1 leading to HCC is crucial to future clinical diagnosis and therapeutic intervention in HCC.

Supplementary Information The online version contains supplementary material available at https://doi.org/10.1007/s13402-025-01044-x.

Acknowledgements The authors would like to thank Professor Jianlin Zhou for providing some reagents and advice. This work was supported by the National Natural Science Foundation of China (No. 81872256), Key grant of research and development in Hunan Province (No. 2020DK2002), Natural Science Foundation in Hunan Province (NO.2021JJ30453), Key project of Hunan Provincial Education Department (No.19A310), Cooperative Innovation Center of Engineering and New Products for Developmental Biology of Hunan Province (No.20134486), as well as City University of Hong Kong Strategic Research Grant (No. 7005264).

Author contributions X.Z. conducted all experiments and prepared all Z.L. and L. L. (Limin Li) conducted animal experiments and data analysis. L.C. conducted cellular and animal experiments. M.O. conducted chIP experiments. H.Z., K.X., L. L. (Ling Lin) conducted animal surgery. C.Z. performed data analysis and interpretation. C.X. performed the exosome extraction. L.Y. performed molecular experiments. W.H. analyzed data. X.D. and L.L. (Limin Li) conceived the conception and design. X.Z. and Z.L. contributed equally to this work.

Data availability No datasets were generated or analysed during the current study.

Declarations

Ethical approval This study was approved by the ethical principles and guidelines for Experiments on Animals and HCC tissues of Hunan Normal University (2018-035).

Patient consent for publication Informed consent for the information to be published was gotten from all patients.

Competing interests The authors declare no competing interests.

References

1. J. Muto, K. Shirabe, K. Sugimachi, Y. Maehara, Review of angiogenesis in hepatocellular carcinoma. Hepatol. Res. **45**(1), 1–9 (2015)
2. H. Sung, J. Ferlay, R.L. Siegel, M. Laversanne, I. Soerjomataram, A. Jemal, F. Bray, Global Cancer statistics 2020: GLOBOCAN estimates of incidence and Mortality Worldwide for 36 cancers in 185 countries. CA Cancer J. Clin. **71**(3), 209–249 (2021)
3. J.M. Llovet, S. Ricci, V. Mazzaferro, P. Hilgard, E. Gane, J.F. Blanc, de A.C. Oliveira, A. Santoro, J.L. Raoul, A. Forner et al., Sorafenib in advanced hepatocellular carcinoma. N Engl. J. Med. **359**(4), 378–390 (2008)
4. X.F. Ding, C. Luo, K.Q. Ren, J. Zhang, J.L. Zhou, X. Hu, R.S. Liu, Y. Wang, X. Gao, J. Zhang, Characterization and expression of a human KCTD1 gene containing the BTB domain, which mediates transcriptional repression and homomeric interactions. DNA Cell. Biol. **27**(5), 257–265 (2008)
5. X. Ding, C. Luo, J. Zhou, Y. Zhong, X. Hu, F. Zhou, K. Ren, L. Gan, A. He, J. Zhu et al., The interaction of KCTD1 with transcription factor AP-2alpha inhibits its transactivation. J. Cell. Biochem. **106**(2), 285–295 (2009)
6. L. Pirone, G. Smaldone, R. Spinelli, M. Barberisi, F. Beguinot, L. Vitagliano, C. Miele, Di S. Gaetano, G.A. Raciti, E. Pedone, KCTD1: a novel modulator of adipogenesis through the interaction with the transcription factor AP2alpha. Biochim. Biophys. Acta Mol. Cell. Biol. Lipids. **1864**(12), 158514 (2019)
7. A.G. Marneros, AP-2beta/KCTD1 control Distal Nephron differentiation and protect against Renal Fibrosis. Dev. Cell. **54**(3), 348–366e345 (2020)
8. D. Hanahan, R.A. Weinberg, The hallmarks of cancer. Cell. **100**(1), 57–70 (2000)
9. S. Tan, L. Xia, P. Yi, Y. Han, L. Tang, Q. Pan, Y. Tian, S. Rao, L. Oyang, J. Liang et al., Exosomal miRNAs in tumor microenvironment. J. Exp. Clin. Cancer Res. **39**(1), 67 (2020)
10. Y. Wang, A. Moh-Moh-Aung, T. Wang, M. Fujisawa, T. Ohara, K.I. Yamamoto, M. Sakaguchi, T. Yoshimura, A. Matsukawa, Exosomal delivery of miR-200b-3p suppresses the growth of hepatocellular carcinoma cells by targeting ERG- and VEGF-mediated angiogenesis. Gene. **931**, 148874 (2024)
11. F.J. Slack, A.M. Chinnaiyan, The role of non-coding RNAs in Oncology. Cell. **179**(5), 1033–1055 (2019)
12. L. Yang, J. Qiu, Y. Xiao, X. Hu, Q. Liu, L. Chen, W. Huang, X. Li, L. Li, J. Zhang et al., AP-2β inhibits hepatocellular carcinoma invasion and metastasis through slug and snail to suppress epithelial-mesenchymal transition. Theranostics. **8**(13), 3707–3721 (2018)
13. O. Menyhart, A. Nagy, B. , Determining consistent prognostic biomarkers of overall survival and vascular invasion in hepatocellular carcinoma. R Soc. Open. Sci. **5**(12), 181006 (2018)
14. W. Huang, Z. Zhong, C. Luo, Y. Xiao, L. Li, X. Zhang, L. Yang, K. Xiao, Y. Ning, L. Chen et al., The miR-26a/AP-2alpha/Nanog signaling axis mediates stem cell self-renewal and temozolomide resistance in glioma. Theranostics. **9**(19), 5497–5516 (2019)
15. W. Huang, C. Chen, Z. Liang, J. Qiu, X. Li, X. Hu, S. Xiang, X. Ding, J. Zhang, AP-2alpha inhibits hepatocellular carcinoma cell growth and migration. Int. J. Oncol. **48**(3), 1125–1134 (2016)

16. X. Ding, Z. Yang, F. Zhou, F. Wang, X. Li, C. Chen, X. Li, X. Hu, S. Xiang, J. Zhang, Transcription factor AP-2alpha regulates acute myeloid leukemia cell proliferation by Hoxa gene expression. Int. J. Biochem. Cell. Biol. **45**(8), 1647–1656 (2013)
17. Y. Wu, Y. Xiao, X. Ding, Y. Zhuo, P. Ren, C. Zhou, J. Zhou, A miR-200b/200c/429-Binding site polymorphism in the 3′ untranslated region of the AP-2α gene is Associated with Cisplatin Resistance. Plos One. **6**(12), e29043 (2011)
18. X. Ding, C. Fan, J. Zhou, Y. Zhong, R. Liu, K. Ren, X. Hu, C. Luo, S. Xiao, Y. Wang et al., GAS41 interacts with transcription factor AP-2beta and stimulates AP-2beta-mediated transactivation. Nucleic Acids Res. **34**(9), 2570–2578 (2006)
19. F. Wang, W. Huang, X. Hu, C. Chen, X. Li, J. Qiu, Z. Liang, J. Zhang, L. Li, X. Wang et al., Transcription factor AP-2beta suppresses cervical cancer cell proliferation by promoting the degradation of its interaction partner beta-catenin. Mol. Carcinog. **56**(8), 1909–1923 (2017)
20. L. Hu, L. Chen, L. Yang, Z. Ye, W. Huang, X. Li, Q. Liu, J. Qiu, X. Ding, KCTD1 mutants in scalp–ear–nipple syndrome and AP–2α P59A in Char syndrome reciprocally abrogate their interactions, but can regulate Wnt/β–catenin signaling. Mol. Med. Rep. **22**(5), 3895–3903 (2020)
21. C. Chen, Z. Liang, W. Huang, X. Li, F. Zhou, X. Hu, M. Han, X. Ding, S. Xiang, Eps8 regulates cellular proliferation and migration of breast cancer. Int. J. Oncol. **46**(1), 205–214 (2015)
22. D.I. Gabrilovich, S. Ostrand-Rosenberg, V. Bronte, Coordinated regulation of myeloid cells by tumours. Nat. Rev. Immunol. **12**(4), 253–268 (2012)
23. Z.W. Zhu, H. Friess, L. Wang, M. Abou-Shady, A. Zimmermann, A.D. Lander, M. Korc, J. M.W. Buchler, Enhanced glypican-3 expression the majority of hepatocellular carcinomas from benign hepatic disorders. Gut. **48**(4), 558–564 (2001)
24. L. Zhou, J. Liu, F. Luo, Serum tumor markers for detection of hepatocellular carcinoma. World J. Gastroenterol. **12**(8), 1175–1181 (2006)
25. J.P. Piret, D. Mottet, M. Raes, C. Michiels, CoCl2, a chemical inducer of hypoxia-inducible factor-1, and hypoxia reduce apoptotic cell death in hepatoma cell line HepG2. Ann. N Y Acad. Sci. **973**(1), 443–447 (2002)
26. D. Chilov, G. Camenisch, I. Kvietikova, U. Ziegler, M. Gassmann, R.H. Wenger, Induction and nuclear translocation of hypoxia-inducible factor-1 (HIF-1): heterodimerization with ARNT is not necessary for nuclear accumulation of HIF-1alpha. J. Cell. Sci. **112**(Pt 8), 1203–1212 (1999)
27. G.L. Semenza, Targeting HIF-1 for cancer therapy. Nat. Rev. Cancer. **3**(10), 721–732 (2003)
28. C.A. Corzo, T. Condamine, L. Lu, M.J. Cotter, J.I. Youn, P. Cheng, H.I. Cho, E. Celis, D.G. Quiceno, T. Padhya et al., HIF-1alpha regulates function and tiation of myeloid-derived suppressor cells in the tumor microenvironment. J. Exp. Med. **207**(11), 2439–2453 (2010)
29. G.L. Wang, B.H. Jiang, E.A. Rue, G.L. Semenza, Hypoxia-inducible factor 1 is a basic-helix-loop-helix-PAS heterodimer regulated by cellular O2 tension. Proc. Natl. Acad. Sci. U.S.A. **92**(12), 5510–5514 (1995)
30. M. Ivan, K. Kondo, H. Yang, W. Kim, J. Valiando, M. Ohh, A. Salic, J.M. Asara, W.S. Lane, W.G. Jr. Kaelin, HIFalpha targeted for VHL-mediated destruction by proline hydroxylation: implications for O2 sensing. Science. **292**(5516), 464–468 (2001)
31. P. Jaakkola, D.R. Mole, Y.M. Tian, M.I. Wilson, J. Gielbert, S.J. Gaskell, von A. Kriegsheim, H.F. Hebestreit, M. Mukherji, C.J. et al., Targeting of HIF-alpha to the Von Hippel-Lindau ubiquitylation complex by O2-regulated prolyl hydroxylation. Science. **292**(5516), 468–472 (2001)
32. Q. Sun, H. Zhou, N.O. Binmadi, J.R. Basile, Hypoxia-inducible factor-1-mediated regulation of semaphorin 4D tumor growth and vascularity. J. Biol. Chem. **284**(46), 32066–32074 (2009)
33. Y.S. Zhang, F.J. Yuan, G.F. Jia, J.F. Zhang, L.Y. Hu, L. Huang, J. Wang, Z.Q. Dai, CIK cells from patients with HCC possess strong cytotoxicity to multidrug-resistant cell line Bel-7402/R. World J. Gastroenterol. **11**(22), 3339–3345 (2005)
34. D. Zhang, H. Lee, Z. Zhu, J.K. Minhas, Y. Jin, Enrichment of selective miRNAs in exosomes and delivery of exosomal miRNAs in vitro and in vivo. Am. J. Physiol. Lung Cell. Mol. Physiol. **312**(1), L110–L121 (2017)
35. M. Zhai, Y. Zhu, M. Yang, C. Mao, Human mesenchymal stem cell derived exosomes enhance cell-free bone regeneration by altering their miRNAs Adv. Sci. (Weinh). **7**(19), 2001334 (2020)
36. A.G. Marneros, A.E. Beck, E.H. Turner, M.J. McMillin, M.J. Edwards, M. Field, de N.L. Macena Sobreira, A.B. Perez, J.A. Fortes, A.K. Lampe et al., Mutations in KCTD1 cause scalp-ear-nipple syndrome. Am. J. Hum. Genet. **92**(4), 621–626 (2013)
37. S. Xu, W. Li, J. Wu, Y. Lu, M. Xie, Y. Li, J. Zou, T. Zeng, H. Ling, The role of miR-129-5p in Cancer: a Novel Therapeutic Target. Curr. Mol. Pharmacol. **15**(4), 647–657 (2022)
38. W. Luo, J. Wang, W. Xu, C. Ma, F. Wan, Y. Huang, M. Yao, H. Zhang, Y. Qu, D. Ye et al., LncRNA RP11-89 facilitates tumorigenesis and ferroptosis resistance through PROM2-activated iron export by sponging miR-129-5p in bladder cancer. Cell. Death Dis. **12**(11), 1043 (2021)
39. S. Ghafouri-Fard, T. Khoshbakht, B.M. Hussen, S.T. Abdullah, M. Taheri, M. Samadian, A review on the role of mir-16-5p in the carcinogenesis. Cancer Cell. Int. **22**(1), 342 (2022)
40. H. Han, W. Li, H. Shen, J. Zhang, Y. Zhu, Y. Li, microRNA-129-5p, a c-Myc negative target, hepatocellular carcinoma progression by blocking the Warburg J. Mol. Cell. Biol. **8**(5), 400–410 (2016)
41. Z. Liu, Y. Wang, L. Wang, B. Yao, L. Sun, R. Liu, T. Chen, Y. Niu, K. Tu, Q. Liu, Long non-coding RNA AGAP2-AS1, functioning as a competitive endogenous RNA, upregulates ANXA11 expression by sponging mir-16-5p and promotes proliferation and metastasis in hepatocellular carcinoma. J. Exp. Clin. Cancer Res. **38**(1), 194 (2019)
42. Y. Zhou, Y. Huang, T. Dai, Z. Hua, J. Xu, Y. Lin, L. Han, X. Yue, L. Ho, J. Lu et al., LncRNA TTN-AS1 sorafenib resistance in hepatocellular carcinoma by sponging mir-16-5p and upregulation of cyclin E1. Biomed. Pharmacother. **133**, 111030 (2021)
43. G.L. Semenza, P.H. Roth, H.M. Fang, G.L. Wang, Transcriptional regulation of genes encoding glycolytic enzymes by hypoxia-inducible factor 1. J. Biol. Chem. **269**(38), 23757–23763 (1994)
44. B.H. Jiang, E. Rue, G.L. Wang, R. Roe, G.L. Semenza, Dimerization, DNA binding, and transactivation properties of hypoxia-inducible factor 1. J. Biol. Chem. **271**(30), 17771–17778 (1996)
45. G. Breier, Functions of the VEGF/VEGF receptor system in the vascular system. Semin Thromb. Hemost. **26**(5), 553–559 (2000)
46. R.S. Apte, D.S. Chen, N. Ferrara, VEGF in Signaling and Disease: Beyond Discovery and Development. Cell. **176**(6), 1248–1264 (2019)
47. P. Saharinen, L. Eklund, K. Pulkki, P. Bono, K. Alitalo, VEGF and angiopoietin signaling in tumor angiogenesis and metastasis. Trends Mol. Med. **17**(7), 347–362 (2011)
48. N. Pore, S. Liu, H.K. Shu, B. Li, D. Haas-Kogan, D. Stokoe, J. Milanini-Mongiat, G. Pages, D.M. O'Rourke, E. Bernhard et al., Sp1 is involved in akt-mediated induction of VEGF expression through an HIF-1-independent mechanism. Mol. Biol. Cell. **15**(11), 4841–4853 (2004)

49. J.A. Forsythe, B.H. Jiang, N.V. Iyer, F. Agani, S.W. Leung, R.D. Koos, G.L. Semenza, Activation of vascular endothelial growth factor gene transcription by hypoxia-inducible factor 1. Mol. Cell. Biol. **16**(9), 4604–4613 (1996)
50. D. Wei, X. Le, L. Zheng, L. Wang, J.A. Frey, A.C. Gao, Z. Peng, S. Huang, H.Q. Xiong, J.L. Abbruzzese et al., Stat3 activation regulates the expression of vascular endothelial growth factor and human pancreatic cancer angiogenesis and metastasis. Oncogene. **22**(3), 319–329 (2003)
51. P.H. Maxwell, M.S. Wiesener, G.W. Chang, S.C. E.C. Vaux, M.E. Cockman, C.C. W C.W. Pugh, E.R. Maher, P.J. The tumour suppressor protein VHL targets hypoxia-inducible factors for oxygen-dependent proteolysis. Nature. **399**(6733), 271–275 (1999)
52. W.G. Kaelin, Von Hippel-Lindau disease. Annu. Rev. Pathol. **2**, 145–173 (2007)
53. C. Ngambenjawong, H.H. Gustafson, S.H. Pun, Progress in tumor-associated macrophage (TAM)-targeted therapeutics. Adv. Drug Deliv Rev. **114**, 206–221 (2017)
54. Z. Li, T. Wu, B. Zheng, L. Chen, Individualized precision treatment: Targeting TAM in HCC. Cancer Lett. **458**, 86–91 (2019)
55. L. D'Ignazio, M. Batie, S. Rocha, Hypoxia and in Cancer, Focus on HIF and NF-kappaB. Biomed. **5**(2) (2017)
56. O.R. Colegio, N.Q. Chu, A.L. Szabo, T. Chu, A.M. Rhebergen, V. Jairam, N. Cyrus, C.E. Brokowski, S.C. Eisenbarth, G.M. Phillips et al., Functional polarization of tumour-associated macrophages by tumour-derived lactic acid. Nature. **513**(7519), 559–563 (2014)
57. J. Baier, M. Gansbauer, C. Giessler, H. Arnold, M. Muske, U. Schleicher, S. Lukassen, A. Ekici, M. Rauh, C. Daniel et al., Arginase impedes the resolution of colitis by altering the microbiome and metabolome. J. Clin. Invest. **130**(11), 5703–5720 (2020)
58. Y. Wang, M. Fu, J. Wang, J. Zhang, X. Han, Y. Song, Y. Fan, K. Hu, J. Zhou, J. Ge, Qiliqiangxin Improves Cardiac Function through Regulating Energy Metabolism via HIF-1alpha-Dependent and Independent Mechanisms in Heart Failure Rats after Acute Myocardial Infarction. Biomed Res Int. **2020**, 1276195 (2020)
59. F. Mouriaux, F. Sanschagrin, C. Diorio, S. Landreville, F. Comoz, E. Petit, M. Bernaudin, A.P. Rousseau, D. Bergeron, M. Morcos, Increased HIF-1alpha expression correlates with cell proliferation and vascular markers CD31 and VEGF-A in uveal melanoma. Investig. Ophthalmol. Vis. Sci. **55**(3), 1277–1283 (2014)
60. L. Liu, Y. Cao, C. Chen, X. Zhang, A. McNabola, D. Wilkie, S. Wilhelm, M. Lynch, C. Carter, Sorafenib blocks the RAF/MEK/ERK pathway, inhibits tumor angiogenesis, and induces tumor cell apoptosis in hepatocellular carcinoma model PLC/PRF/5. Cancer Res. **66**(24), 11851–11858 (2006)
61. W. Chen, Y. Mao, C. Liu, H. Wu, S. Chen, Exosome in Hepatocellular Carcinoma: an update. J. Cancer. **12**(9), 2526–2536 (2021)

Supplemental Figures

Supplemental Figure 1

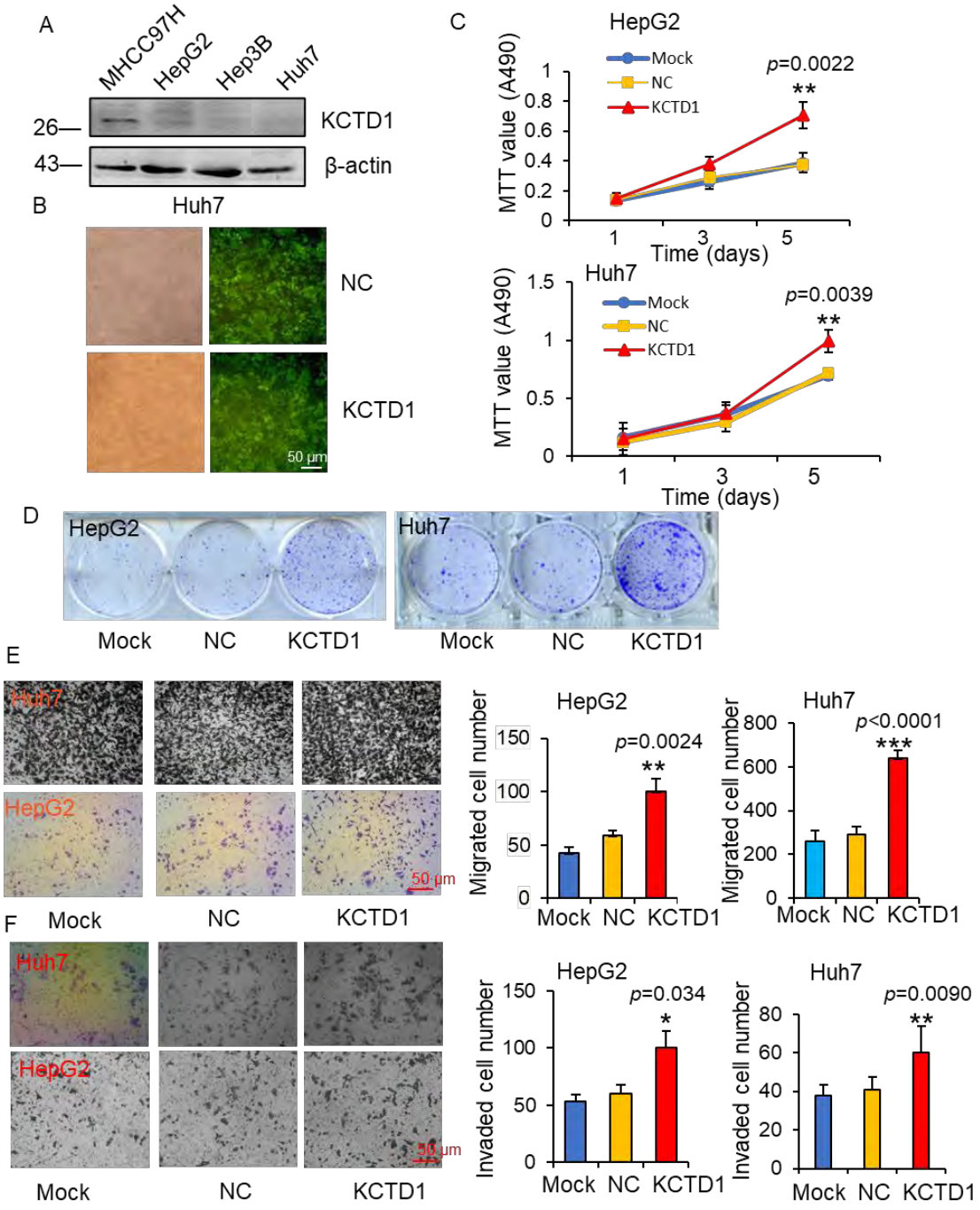

Supplemental Figure 1. KCTD1 overexpression enhancing the *in vitro* growth and invasion of HCC cells. A KCTD1 protein levels in HCC cell lines analyzed by Western blotting. B Immunofluorescence staining of the KCTD1 expression in the

lentiviral-infected Huh7 cells. C MTT analysis of both HCC cell lines infected with KCTD1-LV. D Liquid colony formation assays of the uninfected or LV-infected HCC cells with representative photos taken. E Effects of KCTD1 overexpression on HCC cell migration using transwell migration assays. The average number of migrated HCC cells across the 8-μm pore-size PET membrane was shown. F Effects of KCTD1 overexpression on HCC cell invasion using transwell matrigel invasion assay. The average number of invaded HCC cells was shown. *, $p<0.05$, **, $p<0.01$, and ***, $p<0.001$.

Supplemental Figure 2

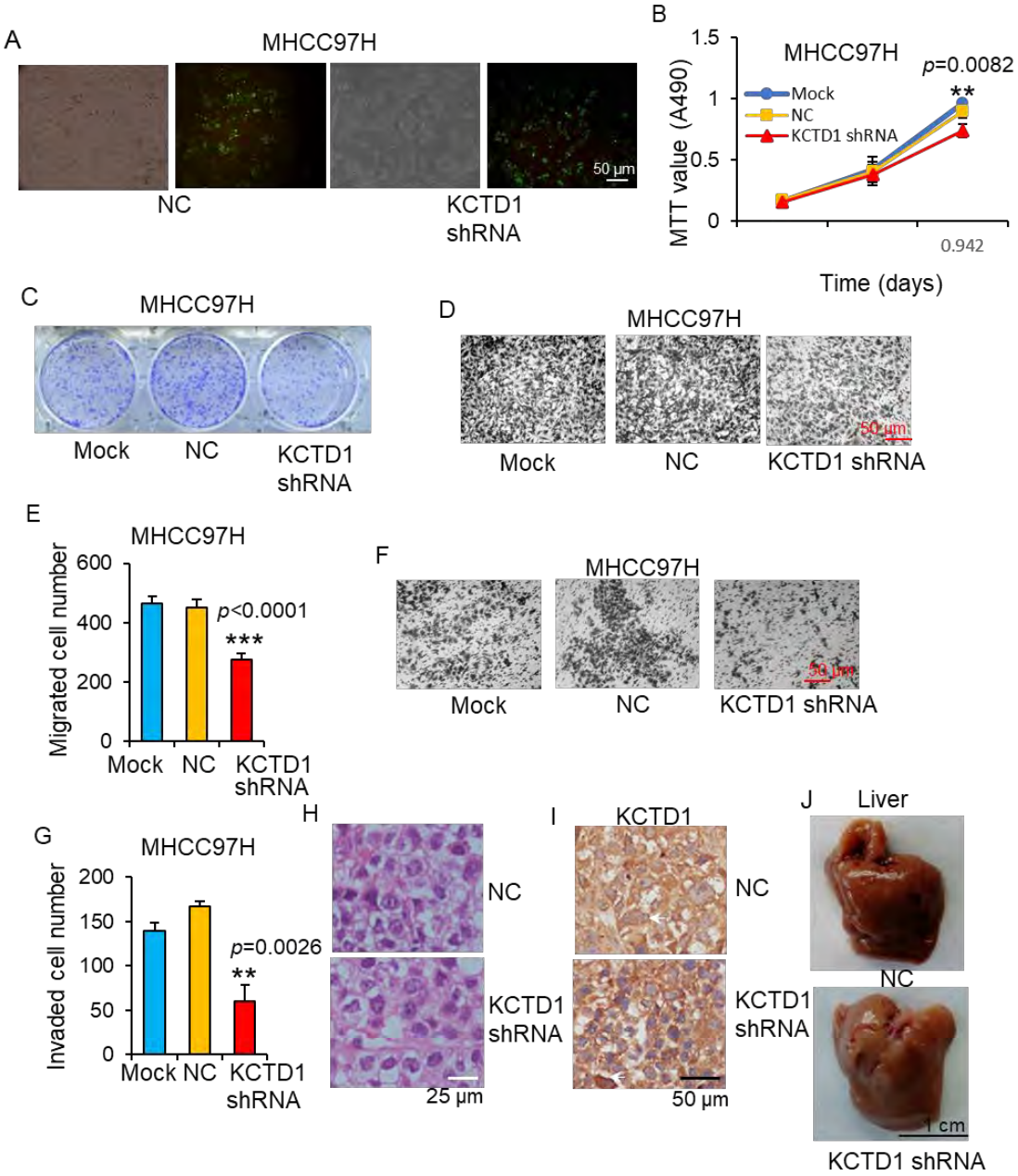

Supplemental Figure 2. KCTD1 knockdown suppressing the *in vitro* and *in vivo* growth, migration and invasion of MHCC97H cells. An Immunofluorescence staining of KCTD1 shRNA in lentiviral-infected MHCC97H cells. B MTT analysis of infected MHCC97H cells. C Representative images of liquid colony formation assays of MHCC97H cells infected with KCTD1 shRNA-LV. D, E Effects of KCTD1 knockdown on MHCC97H cell migration using transwell migration assays with

examples of MHCC97H cells migrating. The average number of migrated MHCC97H cells through the PET membrane was shown. F, G Effects of KCTD1 knockdown on MHCC97H cell invasion with indicated examples of MHCC97H cells migrating through transwell matrigel invasion assays. The average number of invaded MHCC97H cells was shown. H Infected MHCC97H cells injected subcutaneously into the back of nude mice and tumors excised after 2 weeks and analyzed. n=5 mice/group. HE staining carried out on subcutaneous tumors from MHCC97H cells. I IHC staining of KCTD1 expression in MHCC97H tumors. Arrowheads indicate positive staining. J Representative images of the surfaces of the livers. n=5 mice/group. *, $p<0.05$, **, $p<0.01$, and ***, $p<0.001$.

Supplemental Figure 3

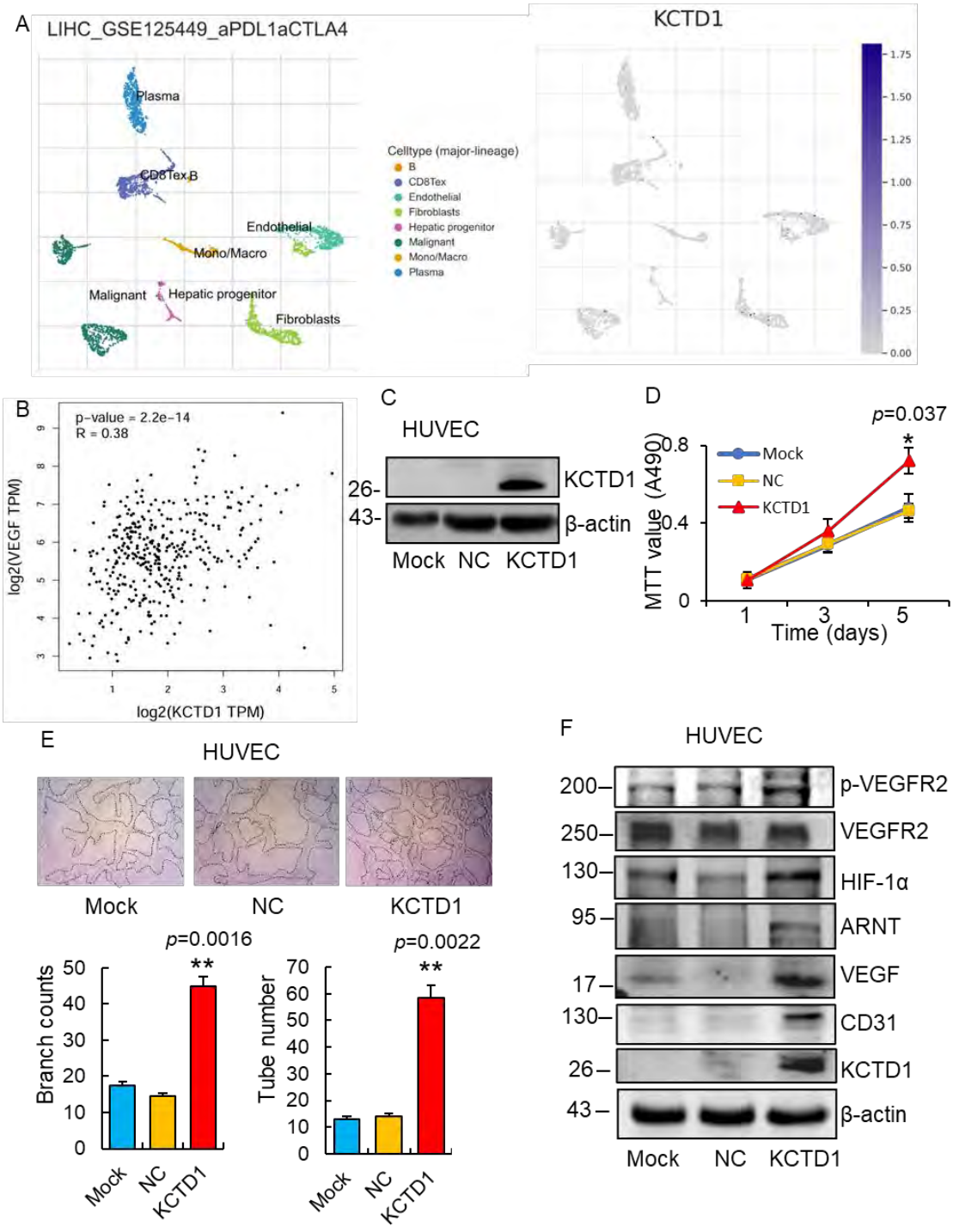

Supplemental Figure 3. Functional analysis of KCTD1 in endothelial cells. A KCTD1 expression was analyzed in HCC by the single-cell RNA sequencing database TISCH (Tumor Immune Single-cell Hub). B TCGA database analysis of the correlation between KCTD1 and VEGF expression. C Western blotting of KCTD1 expression in

infected HUVEC cells with anti-KCTD1 antibodies. D MTT analysis of HUVEC cells infected with KCTD1-LV. E Tube formation capability was detected in KCTD1-overexpressing HUVECs. F Western blot results were shown to investigate the influence of KCTD1 overexpression on the VEGF signaling pathway in HUVECs. *, $p<0.05$, **, $p<0.01$.

Supplemental Figure 4

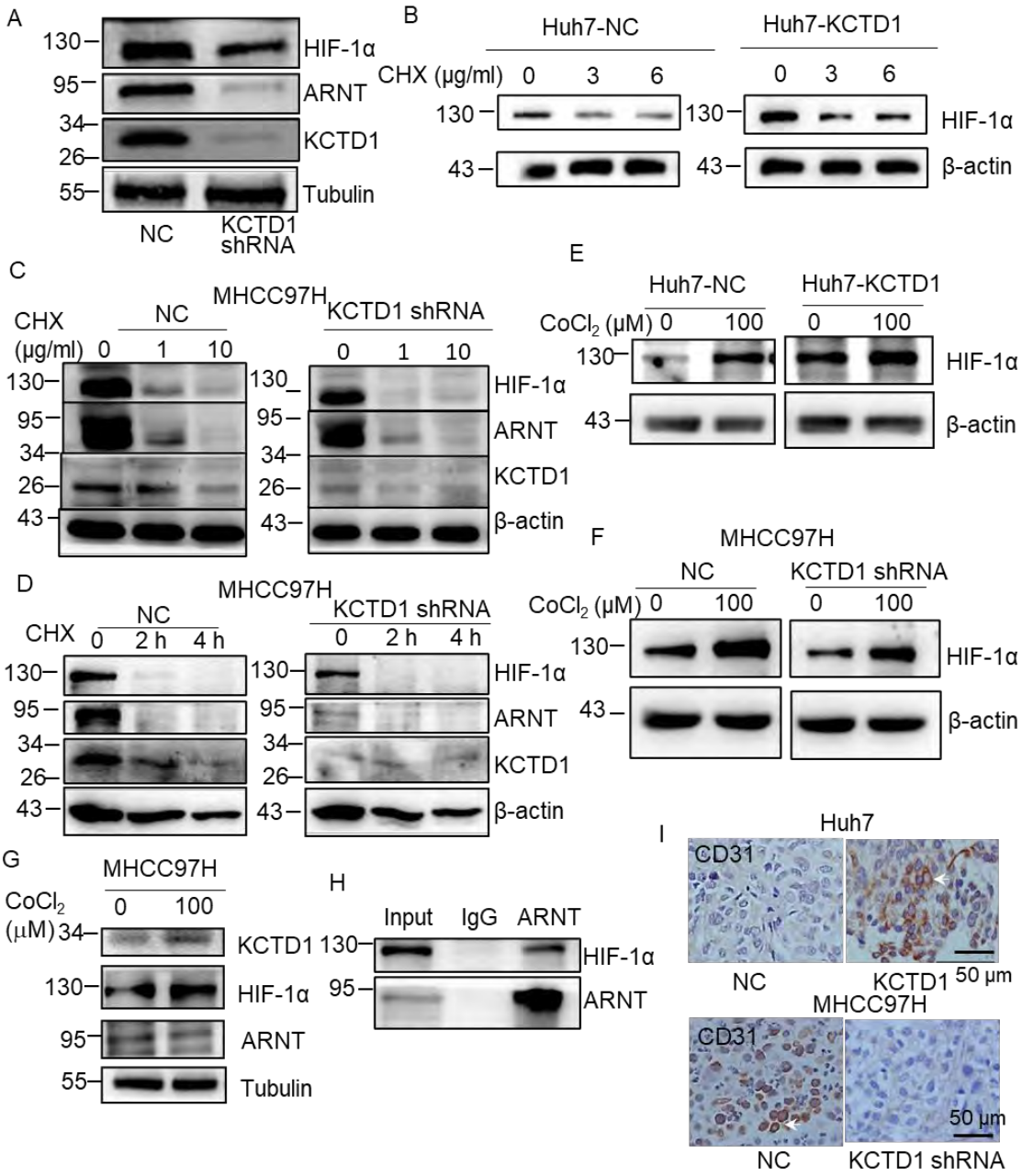

Supplemental Figure 4. Effects of KCTD1 expression on the degradation of HIF-1α protein. A Western blots detecting the expression of KCTD1 and HIF-1α/ARNT in subcutaneous mouse tissues from MHCC97H cells. B Western blots analyzing the expression of HIF-1α protein in KCTD1-overexpressing Huh7 cells under different concentrations of CHX. C, D Western blots detecting the effect of KCTD1 knockdown

on the degradation of HIF-1α/ARNT proteins with the treatment of CHX under different concentrations and different time points. E, F Western blots detecting the influence of KCTD1 overexpression/knockdown on the stability of HIF-1α proteins under hypoxia conditions stimulated by $CoCl_2$. G Western blots detecting the effects of $CoCl_2$ on the expression of KCTD1, HIF-1α and ARNT proteins. H Co-immunoprecipitation analysis performed to demonstrate the interaction HIF-1α and ARNT using ARNT antibodies. I IHC staining of CD31 expression in Huh7 and MHCC97H tumors. Arrowheads indicate positive staining.

Supplemental Figure 5

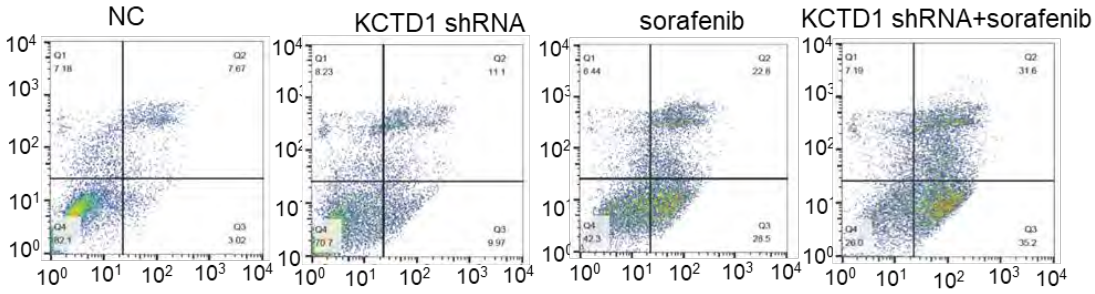

Supplemental Figure 5. Cell apoptosis assays of lentivirus-infected and parental MHCC97H cells treated with sorafenib by flow cytometry and representative results from FACS shown.

Supplemental Figure 6

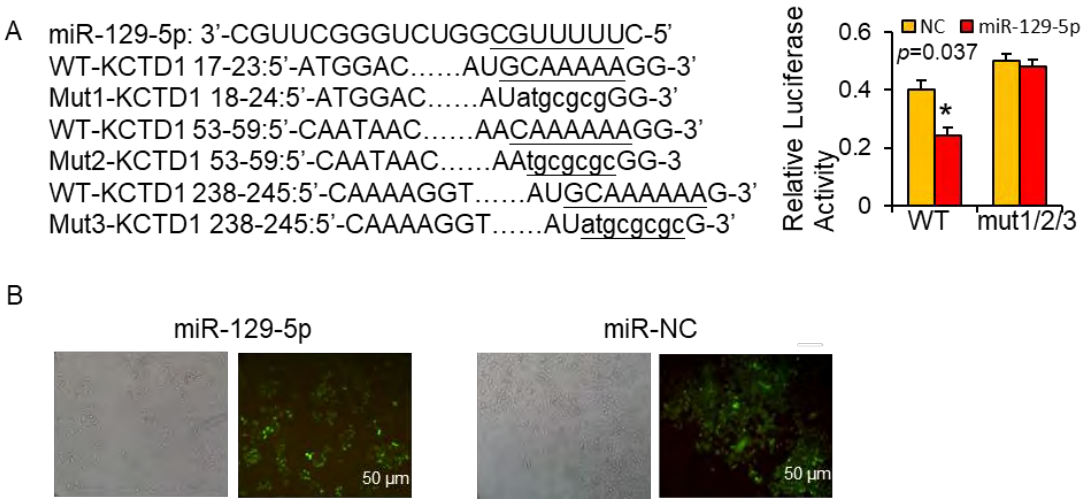

Supplemental Figure 6. miR-129-5p targeting KCTD1 and suppressing HCC progression. A Putative wildtype or mutated luciferase constructs based on the KCTD1 3′ UTR cotransfected with miR-129-5p followed by dual luciferase activity analysis. B Immunofluorescence staining of miR-129-5p lentiviral-infected MHCC97H cells. *, $p<0.05$.

Supplemental Tables

Table S1. Comparisons of KCTD1 expression and the clinical characteristics of HCCs.

Clinical features	**Number**	**Overexpression**	**Low expression**	**P value**
Total number	80			
Sex				**0.03**
Female	8	7	1	
Male	62	26	36	
Age, years（mean，46.5）				0.9493
<46.5	28	15	13	
≥46.5	42	18	24	
Tumor size, cm				0.1821
≤5	48	25	23	
>5	22	8	14	
Cell differentiation				0.2993
Well/ Moderately	47	24	23	
Poor	23	9	14	
Tumor stage				**0.0191**
I/II	50	21	29	
III/IV	20	12	8	
Adjacent normal tissues	10			

Table S2. The clinicopathological parameters of the 70 HCCs and 10 adjacent normal liver tissues used in the study.

Position	No.	Age	Sex	Organ/Anatomic Site	Pathology diagnosis	TNM	Grade	Stage
A1	1	54	F	Liver	Hepatocellular carcinoma	T2N0M0	1	II
A2	2	51	M	Liver	Hepatocellular carcinoma	T2N0M0	1	II
A3	3	42	M	Liver	Hepatocellular carcinoma	T3N0M0	1	III
A4	4	32	M	Liver	Hepatocellular carcinoma	T2N0M0	2	II
A5	5	29	M	Liver	Hepatocellular carcinoma	T3N1M0	2	IVA
A6	6	41	M	Liver	Hepatocellular carcinoma	T2N0M0	2	II
A7	7	58	M	Liver	Hepatocellular carcinoma	T2N0M0	2	II
A8	8	34	M	Liver	Hepatocellular carcinoma	T3N1M0	2	IVA
A9	9	49	M	Liver	Hepatocellular carcinoma	T2N0M0	2	II
A10	10	66	M	Liver	Hepatocellular carcinoma	T2N0M0	2	II
B1	11	47	M	Liver	Hepatocellular carcinoma	T2N0M0	2	II
B2	12	43	M	Liver	Hepatocellular carcinoma	T2N0M0	2	II
B3	13	70	M	Liver	Hepatocellular carcinoma	T2N0M0	3	II
B4	14	44	M	Liver	Hepatocellular carcinoma	T2N0M0	2	II
B5	15	47	M	Liver	Hepatocellular carcinoma	T2N0M0	2	II
B6	16	46	M	Liver	Hepatocellular carcinoma	T2N0M0	2	II
B7	17	36	F	Liver	Hepatocellular carcinoma	T2N0M0	2	II
B8	18	49	M	Liver	Hepatocellular carcinoma	T2N0M0	2	II

B9	19	70	M	Liver	Hepatocellular carcinoma	T3N0M0	2	IIIA
B10	20	48	M	Liver	Hepatocellular carcinoma	T2N0M0	2	II
C1	21	60	M	Liver	Hepatocellular carcinoma	T3N0M0	2	IIIA
C2	22	58	M	Liver	Hepatocellular carcinoma	T3N0M0	2	IIIA
C3	23	42	M	Liver	Hepatocellular carcinoma	T2N0M0	2	II
C4	24	40	M	Liver	Hepatocellular carcinoma	T2N0M0	2	II
C5	25	47	M	Liver	Hepatocellular carcinoma	T3N0M0	2	III
C6	26	78	M	Liver	Hepatocellular carcinoma	T3N0M0	2	IIIA
C7	27	63	F	Liver	Hepatocellular carcinoma	T2N0M0	2	II
C8	28	54	M	Liver	Hepatocellular carcinoma	T4N0M0	2	IIIC
C9	29	62	M	Liver	Hepatocellular carcinoma	T3N0M0	2	III
C10	30	71	M	Liver	Hepatocellular carcinoma	T2N0M0	2	II
D1	31	68	M	Liver	Hepatocellular carcinoma	T2N0M0	2	II
D2	32	44	M	Liver	Hepatocellular carcinoma	T2N0M0	2	II
D3	33	58	M	Liver	Hepatocellular carcinoma	T1N0M0	2	I
D4	34	45	M	Liver	Hepatocellular carcinoma	T2N0M0	2	II
D5	35	66	M	Liver	Hepatocellular carcinoma	T2N0M0	2	II
D6	36	45	M	Liver	Hepatocellular carcinoma	T2N0M0	-	II
D7	37	45	F	Liver	Hepatocellular carcinoma	T2N0M0	2	II
D8	38	41	M	Liver	Hepatocellular carcinoma	T2N0M0	2	II
D9	39	59	M	Liver	Hepatocellular carcinoma	T2N0M0	2	II
D10	40	64	M	Liver	Hepatocellular carcinoma	T2N0M0	2	II

E1	41	65	F	Liver	Hepatocellular carcinoma	T2N0M0	2	II
E2	42	43	M	Liver	Hepatocellular carcinoma	T3N0M0	2	III
E3	43	42	M	Liver	Hepatocellular carcinoma	T3N0M0	2	IIIA
E4	44	42	M	Liver	Hepatocellular carcinoma	T4N0M0	2	IIIC
E5	45	18	M	Liver	Hepatocellular carcinoma	T3N0M0	2	IIIA
E6	46	57	M	Liver	Hepatocellular carcinoma	T2N0M0	2	II
E7	47	56	M	Liver	Hepatocellular carcinoma	T2N0M0	2	II
E8	48	64	M	Liver	Hepatocellular carcinoma	T3N0M0	2	IIIA
E9	49	53	M	Liver	Hepatocellular carcinoma	T2N0M0	2	II
E10	50	34	M	Liver	Hepatocellular carcinoma	T2N0M0	3	II
F1	51	45	M	Liver	Hepatocellular carcinoma with necrosis	T2N0M0	2	II
F2	52	61	M	Liver	Hepatocellular carcinoma	T4N0M0	3	IIIC
F3	53	42	M	Liver	Hepatocellular carcinoma	T2N0M0	3	II
F4	54	48	M	Liver	Hepatocellular carcinoma	T2N0M0	3	II
F5	55	51	F	Liver	Hepatocellular carcinoma	T2N0M0	3	II
F6	56	57	M	Liver	Hepatocellular carcinoma	T2N0M0	3	II
F7	57	32	M	Liver	Hepatocellular carcinoma	T2N0M0	3	II
F8	58	47	M	Liver	Hepatocellular carcinoma	T2N0M0	3	II
F9	59	51	F	Liver	Hepatocellular carcinoma	T2N0M0	3	II
F10	60	46	M	Liver	Hepatocellular carcinoma	T2N0M0	3	II
G1	61	56	M	Liver	Hepatocellular carcinoma	T2N0M0	-	II

G2	62	40	M	Liver	Hepatocellular carcinoma	T4N0M0	3	IIIC
G3	63	63	M	Liver	Hepatocellular carcinoma	T2N0M0	3	II
G4	64	56	M	Liver	Hepatocellular carcinoma	T2N0M0	-	II
G5	65	48	M	Liver	Hepatocellular carcinoma	T3N0M0	-	IIIA
G6	66	35	F	Liver	Hepatocellular carcinoma with necrosis (sparse)	T2N0M0	-	II
G7	67	67	M	Liver	Hepatocellular carcinoma	T2N0M0	3	II
G8	68	60	M	Liver	Hepatocellular carcinoma	T2N0M0	3	II
G9	69	42	M	Liver	Hepatocellular carcinoma	T3N0M0	3	IIIA
G10	70	49	M	Liver	Hepatocellular carcinoma	T3N0M0	3	IIIA
H1	71	63	M	Liver	Liver tissue	-	-	-
H2	72	38	M	Liver	Liver tissue	-	-	-
H3	73	43	M	Liver	Liver tissue	-	-	-
H4	74	48	M	Liver	Liver tissue	-	-	-
H5	75	62	M	Liver	Liver tissue	-	-	-
H6	76	63	F	Liver	Liver tissue	-	-	-
H7	77	65	M	Liver	Liver tissue	-	-	-
H8	78	72	M	Liver	Liver tissue	-	-	-
H9	79	72	M	Liver	Liver tissue	-	-	-
H10	80	38	F	Liver	Liver tissue	-	-	-

Table S3. Primer pairs used in this study.

Name	Sequence (5'- to -3')	Purpose
KCTD1-F	ACGCTAAGCGGTGACAAATCC	RT-PCR
KCTD1-R	CGAGTCGTGATTCCAGCCTG	
KCTD1 3'UTR mut1/2/3-F	CGGTACCATTTCTTAT**atgcgcg**gAACCAA**atatgcgcgc**TAACTCAAA**tgcgcgc**gC	clone
KCTD1 3'UTR mut1/2/3-R	TCGAG**cgcgcgca**TTTGAGTTA**gcgcgcatat**TTGGTT**ccgcgcat**ATAAGAAATGGTACCgagct	
KCTD1 3'UTR WT-F	CGGTACCATTTCTTAT**gcaaaaag**AACCAA**atgcaaaaaa**TAACTCAAA**caaaaaag**C	clone
KCTD1 3'UTR WT-R	TCGAG**ctttttg**TTTGAGTTA**ttttttgcat**TTGGTT**ctttttgc**ATAAGAAATGGTACCgagct	
KCTD1 3'UTR-F	AGCTTTGTTTAAACATGGACATATTTCTTATGCAAA	PCR
KCTD1 3'UTR-R	CCGCTCGAGAATTTCACTTTAATCCAGCCT	
miR-129-5p-RT	GTCGTATCCAGTGCAGGGTCCGAGGTATTCGCACTGGATACGACGCAAGC	RT
miR-129-5p F	CTTTTTGCGGTCTGGGCTTGC	PCR
miR/U6 R	GTGCAGGGTCCGAGGT	
U6-RT	GTCGTATCCAGTGCAGGGTCCGAGGTGCACTGGATACGACAAAATATGG	RT
U6-F	TGCGGGTGCTCGCTTCGGCAGC	PCR
VEGF-chIP F	CAGGAACAAGGGCCTCTGTCT	chIP
VEGF-chIP R	TGTCCCTCTGACAATGTGCCATC	chIP
KCTD1 shRNA F	CcggCGTCCCAGTTCAGCGAATACTCGAGTATTCGCTGAACTGGGACGTTTTTg	clone
KCTD1 shRNA R	aattcaaaaaCGTCCCAGTTCAGCGAATACTCGAGTATTCGCTGAACTGGGACG	
miR-129-5p(upper)	GGAUCUUUUUGCGGUCUGGGCUUGCUGUUCCUCUCAACAGUAGUCAGGAAGCCCUUACCCCAAAAAGUAUCU	clone

Table S4. Correlation between the KCTD1 expression and Arg1 expression in the HCCs by IHC staining.

KCTD1 expression	Cases	Arg1 expression		P value
		Low，No（%）	High，No（%）	
Low（≤30%）	37	19（51.4%）	18（48.6%）	
High（＞30%）	33	15（45.5%）	18（54.5%）	**0.048**
Total	70	34（48.6%）	36（51.4%）	

The KCTD1 and Arg1 expressions are divided into low or high groups according to the IHC score.

Table S5. Correlation between the KCTD1 expression and CD31 expression in the HCCs by IHC staining.

KCTD1 expression	Cases	CD31 expression		P value
		Low，No（%）	High，No（%）	
Low（≤30%）	37	20（54%）	17（46%）	
High（＞30%）	33	10（30%）	23（70%）	**0.0436**
Total	70	30（43%）	40（57%）	

The KCTD1 and CD31 expressions are divided into low or high groups according to the IHC score.